Journal of Neuroscience Research 71:353–364 (2003)

Distinct Protein Kinases Regulate SNAP-25 Expression in Chromaffin Cells

Carmen Montiel,[1] Isabel Mendoza,[2] Carlos J. García,[2] Yusfeye Awad,[2] Jennie García-Olivares,[2] Luisa M. Solís-Garrido,[1] Hernan Lara,[3] Antonio G. García,[1] and Ana M. Cárdenas[2]*

[1]Departamento de Farmacología, Facultad de Medicina, Universidad Autónoma de Madrid, Spain
[2]Cátedra de Farmacología, Escuela de Medicina y Centro de Neurociencia Celular y Molecular de Valparaíso, Universidad de Valparaíso, Chile
[3]Laboratorio de Neurobioquímica, Facultad de Ciencias Químicas y Farmaceúticas, Universidad de Chile, Chile

The contribution of distinct Ca^{2+}-sensitive protein kinases to the regulation of the expression of the synaptosomal-associated protein SNAP-25 was examined in bovine chromaffin cells. Prolonged incubation with high K^+ (38 mM) or 1,1-dimethyl-4-phenyl-piperazinium (DMPP), a nicotinic receptor agonist, significantly increased SNAP-25 protein and mRNA expression, as assessed by immunoblotting and semi-quantitative RT-PCR analysis. Both stimuli preferentially enhanced mRNA coding for the SNAP-25a isoform. Increase of SNAP-25 expression induced by K^+ or DMPP was inhibited over 70% by KN-62 and KN-93, two Ca^{2+}/calmodulin-dependent protein kinase (CaMK) inhibitors, whereas the inactive analogue KN-92 only reduced the expression by 34%. The three compounds also inhibited the high K^+-elicited $[Ca^{2+}]_i$ signal by 40%, suggesting that the effect of KN-62 and KN-93 was a combination of CaMK/ Ca^{2+} influx inhibitory actions. Incubation of the cells with mitogen-activated protein kinase (MAPK) inhibitors PD98059 and U0126 reduced protein expression elicited by high K^+ by 50%, but did not modify the response to DMPP. Interestingly, although protein kinase A (PKA) inhibition by H-89 did not affect the high K^+ or DMPP-induced SNAP-25 expression, basal protein levels were significantly modified upon activation or inhibition of this pathway. Basal expression of SNAP-25 was also modified by the protein kinase C (PKC) activator, phorbol 12-myristate 13-acetate, but not by Gö6976, a PKC-α inhibitor, suggesting that the Ca^{2+}-insensitive PKC-ϵ isoform control basal expression of SNAP-25 in these cells. Taken together, these results provide the first evidence that diverse protein kinases might converge in the induction of SNAP-25 expression in chromaffin cells. The preferential contribution of one or another kinase would depend on the physiological or experimental conditions.

Key words: Ca^{2+} calmodulin-dependent protein kinase; mitogen-activated protein kinase; intracellular Ca^{2+} signals; protein kinase A; protein kinase C

In neurons and neuroendocrine cells, elevations in the concentration of intracellular calcium ($[Ca^{2+}]_i$) in response to different stimuli can trigger diverse and important cellular processes including neurotransmitter release, differentiation, apoptosis and neuronal plasticity. Long-term neuroplasticity is supported by changes in the expression levels of diverse functional proteins (i.e., membrane receptors, biosynthetic enzymes and peptide precursors). These changes in protein levels, which become significant after hours or days of stimulation (Hiremagalur et al., 1993; Bessho et al., 1994; Hiremagalur and Sabban, 1995), could be a consequence of the activation of gene transcription, the stabilization of messenger RNA (mRNA) or the reduction in the rate of protein degradation. All these events can be also controlled by changes in $[Ca^{2+}]_i$.

An example of the diversity of Ca^{2+}-mediated functions can be observed in chromaffin cells from adrenal medulla, a neuroendocrine cell type employed for many years as an experimental model to explore the exocytotic process. In these cells, the increase of $[Ca^{2+}]_i$ elicited by K^+-depolarization or cholinergic receptor activation not only evokes catecholamine secretion but also modulates the expression of several essential proteins, including neuropeptide precursors, enzymes involved in the biosynthesis of catecholamines, and proteins forming part of the exocytotic machinery such as the synaptosomal-associated protein of 25 kDa, SNAP-25 (Stachowiak et al., 1990; Craviso et al., 1992, 1995). Regarding this last protein, its expression is tightly upregulated by a $[Ca^{2+}]_i$ rise in chro-

Contract grant sponsor: Fondecyt (Chile); Contract grant number: 1991018; Contract grant sponsor: DGICYT (Spain); Contract grant number: PB98-0090; Contract grant sponsor: Ministerio de Ciencia y Tecnología (Spain); Contract grant number: SAF 2002-01851; Contract grant sponsor: Programa III PRICIT Grupos Estratégicos de la CAM/UAM (Spain); Contract grant sponsor: Iniciativa Científica Milenio (Chile); Contract grant number: P99-037-F.

*Correspondence to: Ana M. Cárdenas, Cátedra de Farmacología, Escuela de Medicina, Universidad de Valparaíso, Casilla 92-V, Valparaíso, Chile. E-mail: ana.cardenas@uv.cl

Received 18 April 2002; Revised 18 September 2002; Accepted 23 September 2002

maffin cells (García-Palomero et al., 2000a), as occurs in many neuronal cell types; i.e., hippocampal neurons, pituitary cells, granule cells of the dentate gyrus and PC12 cells (Roberts et al., 1998; Sepúlveda et al., 1998; Aguado et al., 1999; Marti et al., 1999; Lee et al., 2000). On the other hand, decreased expression levels of SNAP-25 have been detected in brain of patients with Down syndrome, Alzheimer's disease, or schizophrenia (Young et al., 1998; Greber et al., 1999). Despite the crucial and well-known role of SNAP-25 in the exocytotic event, the signaling pathways underlying the regulation of the its expression in basal or stimulated conditions remain poorly understood.

Reportedly, distinct Ca^{2+}-activated kinase signaling cascades may regulate protein expression. These mechanisms include phosphorylation of transcription factors that activate gene expression (Bading et al., 1993; Bito et al., 1996; Impey et al., 1998), mRNA stabilization (Kaldy and Schmitt-Verhulst, 1995; Lee and Malek, 1998; Park et al., 2001) and protein phosphorylation, which reduces protein degradation (Pasinelli et al., 1995; Dass and Mahalakshmi, 1996; Musti et al., 1997; Turner et al., 1999; Ishida et al., 2000). In hippocampal neurons, Ca^{2+}-calmodulin kinase (CaMK) IV, protein kinase A (PKA) and mitogen-activated protein kinase (MAPK) pathways regulate gene expression by promoting the phosphorylation of the transcription factor CREB, the cyclic AMP-responsive element binding protein (Bito et al., 1996; Impey et al., 1998). In PC12 cells, both protein kinase A (PKA) and protein kinase C (PKC) have been implicated in the nicotine activation of tyrosine hydroxylase and chromogranin A gene expression, respectively (Hiremagalur et al., 1993; Tang et al., 1997). Therefore, it seems likely that the involvement of a protein kinase in the expression of a particular protein depends on the cell type, the protein studied or the stimulus used.

In this study, using immunoblotting, reverse transcription followed by polymerase chain reaction amplification (RT-PCR), $[Ca^{2+}]_i$ recordings and selective protein kinase inhibitors, we have investigated the signaling pathways that regulate SNAP-25 expression in bovine chromaffin cells in basal conditions or upon stimulation with different secretagogues.

MATERIALS AND METHODS

Cell Culture and Treatments

Bovine adrenal chromaffin cells were isolated following standard methods (Livett, 1984), with some modifications (Moro et al., 1990). Cells were suspended in Dulbecco's modified Eagle's medium (DMEM) supplemented with 10% fetal calf serum, 50 IU/ml penicillin and 100 μg/ml gentamicin. Cells (1.2×10^7) were plated on plastic culture dishes (10-cm diameter) at a density of 10×10^6 cells/ml. In the case of cytosolic Ca^{2+} experiments, cells were plated on glass coverslips (25-mm diameter) at a density of 2.5×10^4 cells/ml. Cells were kept in a water-saturated incubator at 37°C, in a 5% CO_2/95% air atmosphere. To activate SNAP-25 mRNA or protein expression, cells were incubated with 38 mM KCl or 20 μM 1,1 dimethyl-4-phenylpiperazinium (DMPP) during 24 hr or 48 hr, respectively, as described previously (García-Palomero et al., 2000a). To obtain a final concentration of 38 mM KCl, 2 ml of an osmotically balanced stock high-K^+ solution (170 mM KCl, 0.9 mM $CaCl_2$, 1.3 mM $MgCl_2$, 10 mM HEPES, pH 7.4) were added to 8 ml of DMEM. Controls, non-stimulated cells, were manipulated as experimental cells, but were incubated in a medium in which high KCl was replaced with NaCl. To evaluate the effect of protein kinase inhibitors, cells were incubated with KN-62, KN-93, KN-92, PD98059, H-89 (all from Calbiochem, Darmstadt, Germany) or U0126 (Promega, Madison, WI) 15 min before and during the entire stimulation period with K^+ or DMPP. For experiments with Gö6976 (Calbiochem), cells were incubated with this inhibitor 1 hr before and during the entire stimulation period. To determine the effect of PKC or PKA activation on SNAP-25 levels, cells were incubated with phorbol 12-myristate 13-acetate (PMA), dibutyryl-cAMP (db-cAMP), 1,9 dideoxyforskolin or forskolin (all from Sigma, St. Louis, MO) during 48 hr.

Immunoblot Analysis

Equal amounts of cell lysate proteins (typically 40 μg total proteins) were separated by polyacrylamide gel electrophoresis using the Laemmli buffer system (Laemmli, 1970). Proteins were transferred electrophoretically to nitrocellulose membranes by standard procedures. Membranes were incubated for 2 hr with a monoclonal anti-SNAP-25 antibody (Sternberger Monoclonals Inc.), diluted 1:1,000 in Tris-buffer solution (NaCl 150 mM, KCl 2.8 mM, Tris-HCl 25 mM, pH 7.4), at room temperature. A monoclonal antibody against β-actin (1:1,000; Sigma) was also used as internal control in all experiments to make sure that equal amounts of protein were charged and transferred to the membrane. After washing, membranes were incubated for 1 hr with a secondary antibody labeled with horseradish peroxidase and revealed using the enhanced chemiluminescence detection system (Pierce, Rockford, IL). To compare changes in the expression of SNAP-25, the autoradiographs were scanned; density and area of each band were determined with the NIH Image 1.6 program (García-Palomero et al., 2000a). The relationship between different amounts of SNAP-25 and the area of each band given by the software gave a correlation index of 0.989 (data not shown).

Intracellular Ca^{2+} Measurements

Variations in $[Ca^{2+}]_i$ were determined by microfluorometry, as described previously (Cárdenas et al., 2002). Cells plated in coverslips were incubated with 10 μg/ml Indo-1 acetoxymethylester (Molecular Probes, Eugene, OR) at 37°C for 40 min, and later washed with Krebs-HEPES (pH 7.4). The coverslips were then mounted in a perfusion chamber, which was placed on the stage of a fluorescence-inverted microscope (Diaphot-200, Nikon Corp.) equipped with two dichroic mirrors. One dichroic mirror was used to send the excitation light (355 nm) to the cells and the fluorescent light emitted by Indo-1 inside the cells (>400 nm) to the second mirror. The second dichroic mirror was used to split the fluorescent light into beams of light centered at 410 and 485 nm, respectively. The intensity of the light at each wavelength was measured continuously using two photomultipliers, and the analog signal was digitized using an A/D converter board (Labmaster, Micro Systems) installed in a dedicated PC compatible computer. Digital data was captured and stored in the hard disk for analysis. A computer program

calculated the F410/F485 ratio and yielded the corresponding $[Ca^{2+}]_i$ from a calibration curve obtained using a calcium calibration buffer kit (Molecular Probes)

RT-PCR Analysis

Total RNA was extracted from cultured bovine adrenomedullary chromaffin cells, as described previously (García-Palomero et al., 2000b), using the Ultraspec RNA isolation kit (Biotecx Laboratories, East Houston, TX). cDNA was synthesized from 1 μg of total RNA using the Moloney murine leukemia virus (M-MLV) reverse transcriptase (Gibco/BRL). The PCR was carried out in 50 μl of reaction sample containing cDNA (corresponding to 10–50 ng of total RNA), 10 pmol of each oligonucleotide primer, 200 μM of dNTP and 2.5 U of Taq polymerase (Qiagen, Hilden, Germany). The PCR reaction was carried out using 28 cycles (denaturation at 94°C for 45 sec, annealing at 60°C for 60 sec, and elongation at 72°C for 60 sec), followed by an additional polymerization at 72°C for 120 sec. Three different products were amplified, using specific primers based on the nucleotide sequence of the rat SNAP-25, according to Grant et al. (1999). The first product (559 bp), corresponding to the cDNA coding for both SNAP-25 isoforms and referred to as "total SNAP-25" was amplified with a forward primer on exon 2 and a reverse primer on exon 7/8. For the isoform-specific PCRs, amplified products corresponding to the SNAP-25a or SNAP-25b isoforms (both with a size of 202 bp) were obtained by replacing the above reverse primer with the exon 5a or exon 5b, respectively. The following set of primers (from 5′–3′) were used; numbers in brackets indicate the accession number of the sequence: Total SNAP-25 [AB003991] exon 2, forward: 5′-AGGACGCAGACATGCGTAATG-AACTGGAGG-3′, exon 7/8, reverse: GTTGGAGTCAGC-CTTCTCCATGATCCTGTC; SNAP-25a [AB003991] Exon 5a, reverse: TTGGTTGATATGGTTCATGCCTTCTTC-GACACGA; SNAP-25b [AB003992] Exon 5b, reverse: CTTATTGATTTGGTCCATCCCTTCCTCAATGCG. For semi-quantitative analysis of SNAP-25 mRNA, RT-PCR amplification of mRNA corresponding to β-actin was carried out routinely in parallel as an internal control of messenger quality and quantity. Primers selected for the amplification of β-actin from bovine chromaffin cells were designed from the nucleotide sequence of human β-actin; numbers in brackets indicate accession number (before) and initial position of the primer (after) the sequence: [X00351]. Forward: AACGGCTCCGGCAT-GTGC (75); reverse: GGTCTCAAACATGATCTGGG (419). In addition, RT-PCR carried out in the absence of M-MLV reverse transcriptase was used in all cases to rule out a potential contamination of genomic DNA. PCR samples were run on a 1.5% agarose gel, using a 100-bp DNA ladder as molecular weight marker (Biotools, B&M Labs, Spain). The product amplified from total SNAP-25 was extracted from the gel using the Geneclean Kit (Qiagen), according to the manufacturer's instructions. Sequencing of this product was carried out using the Big Dye method and the automatic sequencer ABI PRISM 377 (Perkin-Elmer). To determine changes in the expression of mRNA SNAP-25, the density and area of each band of the SNAP-25 PCR products were analyzed with the NIH Image 1.6 program and values were normalized to the densitometric values of the corresponding β-actin PCR products. It is noteworthy that under the above experimental conditions, the number of PCR cycles was selected so that in all cases, the amplified signals are in the dynamic range (not saturated).

Data Analysis

Values of protein expression induced by high K^+ or DMPP were expressed as mean ± SEM of the relative increment of SNAP-25 expression in stimulated cells compared to non-stimulated cells (considered as the unit). In the case of experiments assaying the effects of kinase inhibitors, data were expressed as percent of blockade of the response elicited by high K^+ or DMPP (referred as 100%), and they represent the mean ± SEM values obtained in different batches of cells. The statistical significance of the differences was evaluated using one-way ANOVA. A level of $P < 0.05$ was considered statistically significant.

RESULTS

Effects of CaMK Inhibitors on SNAP-25 Expression Induced by High K^+ Depolarization of Chromaffin Cells

Two CaMK inhibitors, KN-62 and KN-93, were used to evaluate the role of this Ca^{2+}-activated protein kinase in the control of SNAP-25 expression elicited by depolarization of chromaffin cells. Both compounds act as CaMK-II inhibitors (Niki et al., 1993), although they also interfere with other CaMK isoforms (Bito et al., 1996).

Depolarization of cells with high KCl, as described in Methods, increased the SNAP-25 protein levels by 2.5 ± 0.4-fold ($n = 7$, $P < 0.01$) referred to control non-stimulated cells (Fig. 1A). Inset of Figure 1A shows a typical immunoblot of SNAP-25 protein expression (25 kDa) using β-actin (42 kDa) as internal control. Changes in the protein expression were also observed at the mRNA level, as assessed by semi-quantitative analysis of PCR products corresponding to total SNAP-25 mRNA in control or stimulated cells (Fig. 1B). Results also indicated that although both isoforms of SNAP-25 are expressed in basal conditions, mRNA encoding for the SNAP-25a isoform in particular seems increased upon depolarization (Fig. 1B). The densitometry analysis of the PCR products revealed that cell depolarization increased SNAP-25a mRNA levels by 1.8 ± 0.13-fold ($P < 0.01$) referred to non-treated control cells (Fig. 1C).

Incubation of cells with KN-62 (10 μM) or KN-93 (10 μM) inhibited the increase in SNAP-25 expression induced by depolarization by 70 ± 9% ($n = 7$) and 88 ± 11% ($n = 5$), respectively (Fig. 2A). These results were compared to those obtained in the presence of KN-92 (10 μM), a structural analogue of KN-93 that does not have inhibitory activity on CaMK. Although KN-92 reduced the protein expression induced by high K^+ by 34 ± 10%, this effect was significantly lower than that obtained with KN-93 ($P < 0.01$) and KN-62 ($P < 0.05$). Figure 2B shows a representative immunoblot of these experiments. It should also be mentioned that the incubation of chromaffin cells with these compounds during 48 hr did not affect the basal levels of SNAP-25 (data not shown).

The inhibitory effect of KN-93 on protein expression was also observed at the mRNA level. Thus, whereas

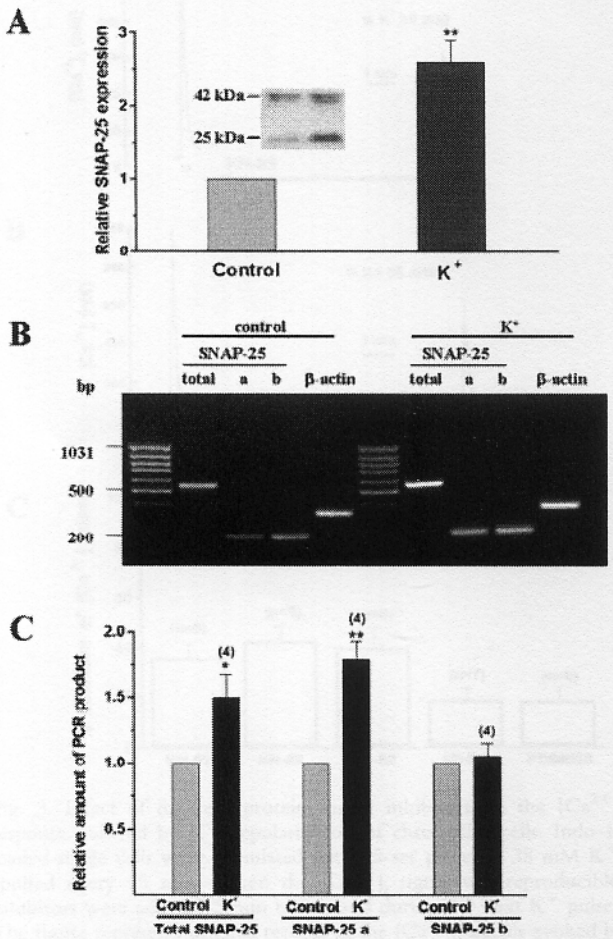

Fig. 1. Depolarization increased SNAP-25a isoform in bovine chromaffin cells. Cells were incubated for 24 hr (for mRNA analysis) or 48 hr (for protein analysis) in control conditions or in the presence of 38 mM KCl. **A:** Relative increment of SNAP-25 protein expression observed in cells treated with high K^+, compared to non-stimulated control cells. Data are mean ± SEM values obtained in seven different batches of cells. $^{**}P < 0.01$. The inset shows a representative immunoblot of the SNAP-25 (25 kDa) and β-actin (42 kDa) protein expression levels in control (C) or in depolarized cells (K^+). **B:** Relative expression of mRNAs corresponding to "total SNAP-25" or its isoforms, in control or K^+-depolarized chromaffin cells. mRNA levels were determined by semi-quantitative RT-PCR analysis, using β-actin mRNA as internal control. Total RNA was extracted from each cell batches, then RT and parallel PCRs were carried out using selective primers. Aliquots (20 μl) of each PCR reaction were run on 1.5% agarose gel and stained with ethidium bromide to identify the bands corresponding to total SNAP-25 (559 bp), isoform-a (202 bp), isoform-b (202 bp) and β-actin (344 bp). **C:** SNAP-25 mRNA levels (in arbitrary units) were quantified by densitometric scanning of ethidium bromide stained PCR products and normalized to the densitometric values of the corresponding β-actin PCR products. Data are mean SEM values obtained in three independent experiments. $^{*}P < 0.05$, $^{**}P < 0.01$.

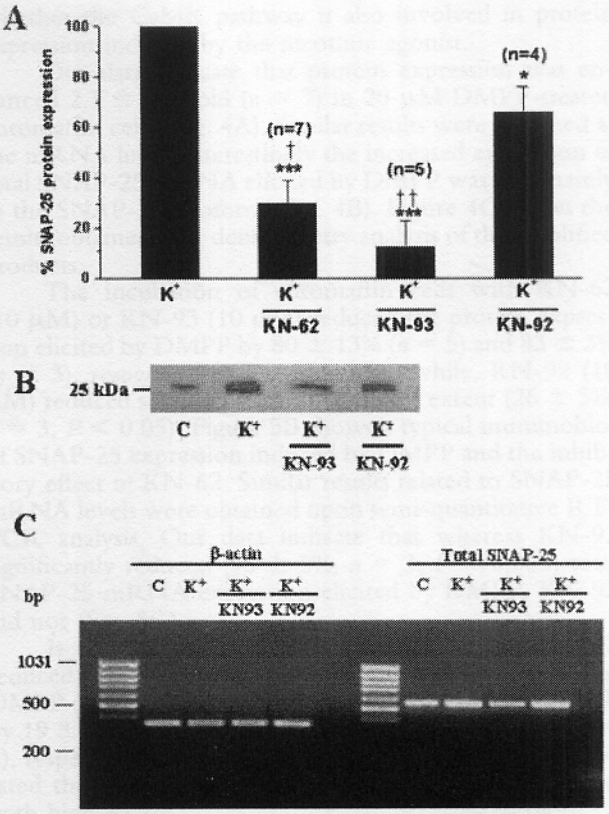

Fig. 2. CaMK inhibitors reduce the increase of SNAP-25 protein and mRNA expression induced by high K^+. Cells were incubated with 38 mM KCl for 24 or 48 hr, in the absence or presence of KN-62, KN-93 or its inactive analogue, KN-92. Inhibitors at a concentration of 10 μM were present 15 min before and during the entire depolarization period. **A:** Values are expressed as percentage of the protein expression elicited by high K^+ (defined as 100%). Data are mean ± SEM values obtained from the number of batches of cells shown in parentheses. $^{***}P < 0.001$, $^{*}P < 0.05$ compared to K^+ values in the absence of inhibitors; $^{\dagger\dagger\dagger}P < 0.001$, $^{\dagger}P < 0.05$ compared to KN-92. **B:** Representative immunoblot of SNAP-25 expression in control (C) and depolarized cells (K^+) in the absence or presence of KN-93 or KN-92. **C:** RT-PCR analysis shows that CaMK inhibition with KN-93 prevents the increase of total SNAP-25 mRNA levels induced by high K^+, whereas the inactive CAMK inhibitor, KN-92 (10 μM), did not modify the SNAP-25 mRNA expression levels. Figure shows a typical experiment from the three carried out with total RNAs extracted from different cell batches. In parallel, results are shown of the PCR products corresponding to β-actin.

high K^+ enhanced the total SNAP-25 mRNA level 2.3 ± 0.22-fold, KN-93 inhibited the increase by 83.5 ± 16% ($P < 0.01$, n = 3); in contrast, KN-92 did not significantly modify the amplified SNAP-25 PCR product.

Because the effect of KN-92 on the SNAP-25 protein expression could be the consequence of its well documented Ca^{2+} channel blockade effect (Maurer et al., 1996; Tsutsui et al., 1996), we assayed the effect of KN-92, KN-93, and KN-62 on the $[Ca^{2+}]_i$ response induced

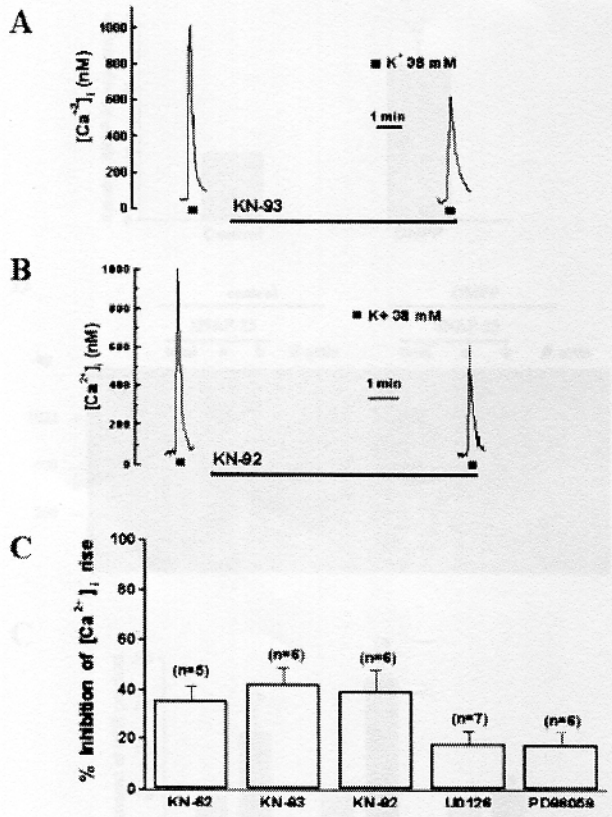

Fig. 3. Effect of different protein kinase inhibitors on the $[Ca^{2+}]_i$ response induced by K^+ depolarization of chromaffin cells. Indo-1-loaded single cells were stimulated with 15-sec pulses of 38 mM K^+, applied every 15 min. When the $[Ca^{2+}]_i$ signal was reproducible, inhibitors were added (15 min before and during the next K^+ pulse). The figure represents original records of the $[Ca^{2+}]_i$ signals evoked by two successive K^+ pulses (black squares at the bottom of the panel), in the absence or presence of KN-93 (A) or KN-92 (B). C: Inhibitory effect of different protein kinase inhibitors on the $[Ca^{2+}]_i$ rise evoked by K^+ pulses applied as described above. Data, expressed as percentage of inhibition of the response mediated by K^+ in the absence of inhibitors (100%), are mean ± SEM values obtained in the number of cells shown in parentheses.

by 38 mM K^+. For these experiments, Indo-1-loaded single chromaffin cells were stimulated with successive 15-sec pulses of high K^+, applied every 15 min. After two or three initial pulses, when $[Ca^{2+}]_i$ signals were reproducible, KN-62, KN-93 and KN-92 were added 15 min before and during the next K^+ pulse (Fig. 3A,B). Figure 3C shows how the $[Ca^{2+}]_i$ signal was inhibited below 40% by the three agents assayed.

Effect of CaMK Inhibitors on SNAP-25 Expression Elicited by DMPP Treatment of Chromaffin Cells

Because incubation of chromaffin cells with DMPP induces the increase of SNAP-25 protein expression, as high K^+ does (García-Palomero et al., 2000a), we studied whether the CaMK pathway is also involved in protein expression induced by the nicotinic agonist.

Our data indicate that protein expression was enhanced 2.3 ± 0.5-fold ($n = 7$) in 20 μM DMPP-treated chromaffin cells (Fig. 4A). Similar results were obtained at the mRNA level; interestingly the increased expression of total SNAP-25 mRNA elicited by DMPP was due mainly to the SNAP-25a isoform (Fig. 4B). Figure 4C shows the results obtained after densitometry analysis of the amplified products.

The incubation of chromaffin cells with KN-62 (10 μM) or KN-93 (10 μM) reduced the protein expression elicited by DMPP by 80 ± 13% ($n = 5$) and 83 ± 3% ($n = 3$), respectively (Fig. 5A). Meanwhile, KN-92 (10 μM) reduced such expression to a lesser extent (26 ± 3%, $n = 3$; $P < 0.05$). Figure 5B shows a typical immunoblot of SNAP-25 expression induced by DMPP and the inhibitory effect of KN-62. Similar results related to SNAP-25 mRNA levels were obtained upon semi-quantitative RT-PCR analysis. Our data indicate that whereas KN-93 significantly reduced (95 ± 5%, $n = 3$; $P < 0.005$) total SNAP-25 mRNA expression elicited by DMPP, KN-92 did not (Fig. 5C).

It is noteworthy that KN-62, KN-93 and KN-92 reduced the $[Ca^{2+}]_i$ signals generated by brief pulses of DMPP (15-sec, 20 μM) applied to single chromaffin cells by 19 ± 7% ($n = 4$), 28 ± 9% ($n = 3$) and 24 ± 8% ($n = 5$), respectively (not shown). These last findings corroborated the results obtained previously in cells depolarized with high KCl.

Effects of MAPK Inhibition on SNAP-25 Expression Elicited by High K^+ or DMPP

To examine the role of MAPK in the control of SNAP-25 expression, we used two inhibitors, PD98059 and U0126. It has been described that both agents block MAPK kinase (MEK), but whereas PD98059 inhibits only the inactive MEK, U0126 inhibits both active and inactive MEK (Favata et al., 1998). Our results indicate that none of these inhibitors has significant effects on basal or DMPP-induced SNAP-25 expression ($n = 3$; data not shown). In contrast, PD98059 (50 μM) and U0126 (10 μM) reduced (by 46 ± 11% and 59 ± 15%, respectively) the high K^+-induced SNAP-25 expression (Fig. 6A). The inhibitory effect of U0126 was also reproduced at the mRNA level (Fig. 6C). The densitometry analysis of the PCR products showed that K^+-depolarization increased by 2.65 ± 0.22-fold ($n = 4$; $P < 0.001$) total SNAP-25 mRNA level; the increase was inhibited by 65.7 ± 13% in the presence of U0126 ($n = 4$, $P < 0.05$). Additionally, following protocols similar to those described previously for other kinase inhibitors in Indo-1 loaded cells, we found that PD98059 and U0126 slightly reduced (by 20%) the $[Ca^{2+}]_i$ rise elicited by 38 mM KCl (Fig. 3C).

When CaMK and MAPK inhibitors were assayed together on the SNAP-25 protein expression induced by high K^+, we observed that the response to depolarization was almost abolished; the inhibition reached a value of 88 ± 9% for KN-62 plus PD98059, and 89 ± 10% for the

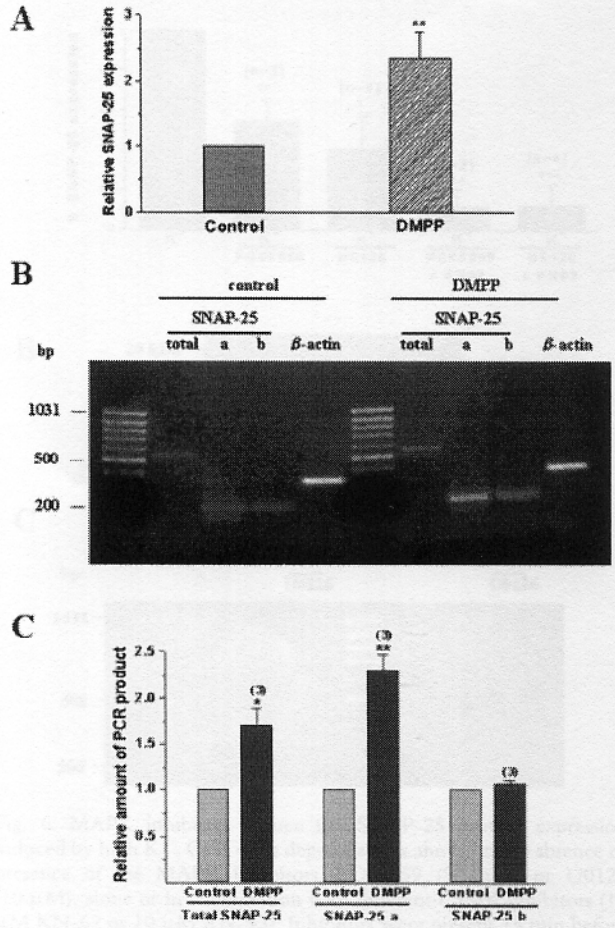

Fig. 4. Nicotine receptor activation with DMPP increased SNAP-25a isoform in bovine chromaffin cells. Cells were incubated for 24 hr (for mRNA analysis) or 48 hr (for protein analysis) in control conditions or in the presence of the nicotine receptor agonist, DMPP. **A:** Relative increment of SNAP-25 protein expression obtained in cells treated with DMPP, compared to non-stimulated control cells. Data are mean ± SEM values obtained with seven different cell batches. $^{**}P < 0.01$. **B:** Relative expression of mRNA levels corresponding to total SNAP-25 and to each of its isoforms, in control and in DMPP-stimulated chromaffin cells. mRNA levels were determined by RT-PCR assay, as described previously for KCl depolarization, but in these experiments, cells were incubated with DMPP (20 μM) over 24 hr. PCR amplification of mRNA corresponding to β-actin was carried out routinely, in parallel. Aliquots (20 μl) of each PCR reaction were run on 1.5% agarose gels and stained with ethidium bromide to visualize the SNAP-25 (559 bp), isoform-a (202 bp), isoform-b (202 bp) and β-actin (344 bp) bands. **C:** SNAP-25 mRNA levels (in arbitrary units) were quantified by densitometric scanning of ethidium bromide-stained PCR products and normalized to the densitometric values of the corresponding β-actin PCR products. Data are mean ± SEM values obtained in three independent experiments. $^{*}P < 0.05$, $^{**}P < 0.01$.

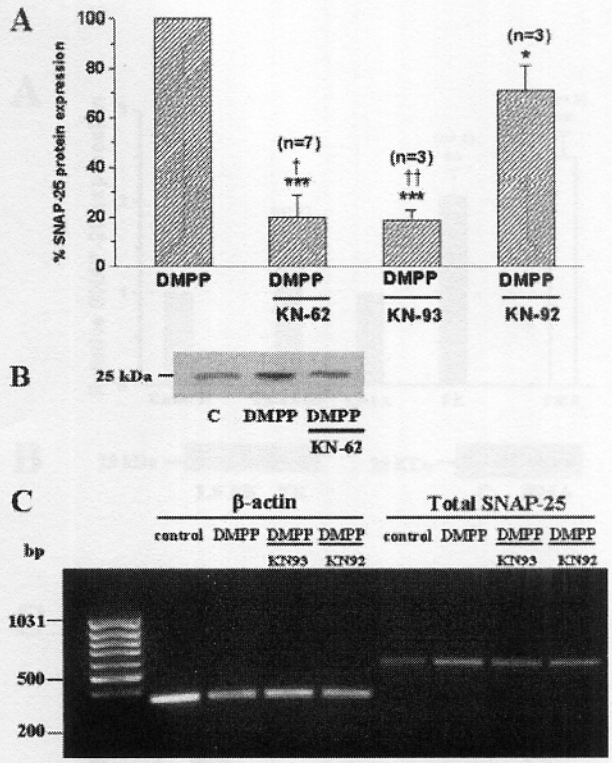

Fig. 5. CaMK inhibitors reduce the increase of SNAP-25 protein and mRNA expression induced by DMPP. Cells were incubated with the nicotinic receptor agonist DMPP (20 μM) for 24 or 48 hr, in the absence or presence of KN-62, KN-93 or its inactive analogue KN-92, all of them at 10 μM **A:** Blockade of the SNAP-25 protein expression elicited by DMPP (defined as 100%) by different inhibitors. Data are mean ± SEM values. The number of experiments is shown in parentheses. $^{***}P < 0.001$, $^{*}P < 0.05$ compared to K^+ values in the absence of inhibitors; $^{†††}P < 0.001$, $^{†}P < 0.05$ compared to the KN-92 inhibitory effect. **B:** A typical immunoblot of SNAP-25 expression in control non-stimulated cells (C) or in DMPP-treated cells in the absence or presence of KN-62. **C:** RT-PCR analysis of total SNAP-25 and β-actin in non-stimulated cells (control), or in DMPP-treated cells in the absence or presence of KN-93 or KN-92. Aliquots (20 μl) of each PCR reaction were run on 1.5% agarose gels and stained with ethidium bromide to visualize the bands.

combination of KN-93 plus U0126 (Fig. 6A). Figure 6B shows a typical immunoblot of the protein expression induced by high K^+, and the effects of PD98059, and PD98059 plus KN-62.

Effects of PKA Inhibition and Activation on SNAP-25 Protein Expression

To investigate the contribution of PKA in the control of SNAP-25 expression in chromaffin cells, we assayed the effect of one inhibitor and two activators of this kinase. In these batches of cells, the relative increase of SNAP-25 expression induced by high K^+ (38 mM) or DMPP (20 μM) was 2.5 ± 0.3-fold ($n = 4$, $P < 0.01$) and 1.7 ± 0.1-fold ($n = 5$, $P < 0.01$), respectively, compared to non-stimulated control cells. The PKA inhibitor H-89 (10 μM) did not affect SNAP-25 expression induced by high K^+ or DMPP (data not shown).

In contrast, the incubation of cells with the PKA activator db-cAMP (1 mM, 48 hr), promoted a significant

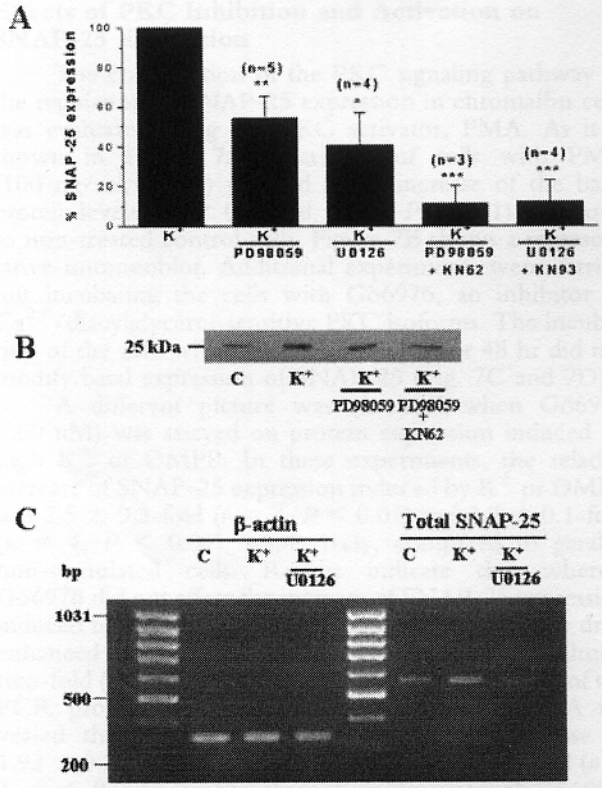

Fig. 6. MAPK inhibitors reduce the SNAP-25 protein expression induced by high K^+. Cells were depolarized as above, in the absence or presence of the MAPK inhibitors, PD98059 (50 μM) or U0126 (10 μM), alone or in combination with different CaMK inhibitors (10 μM KN-62 or 10 μM KN-93). Inhibitors were present 15 min before and throughout the entire depolarization period. **A:** Effect of MAPK inhibitors expressed as a percentage of the SNAP-25 expression induced by high K^+ (defined as 100%). Data are mean ± SEM values. The number of experiments is shown in parentheses. $***P < 0.001$, $*P < 0.05$ compared to K^+ values in the absence of inhibitors. **B:** Representative immunoblot of SNAP-25 revealing that the MAPK inhibition reduces the SNAP-25 protein expression induced by high K^+. Control band (C) represents the protein expression in non-stimulated cells. **C:** RT-PCR analysis of the effect of U0126 (10μM) on mRNA expression levels for SNAP-25 and β-actin induced by KCl (38 mM, 24 hr). Aliquots of each PCR reaction were run on 1.5% agarose gels and stained with ethidium bromide to visualized the total SNAP-25 (559 bp) and β-actin (344 bp) bands.

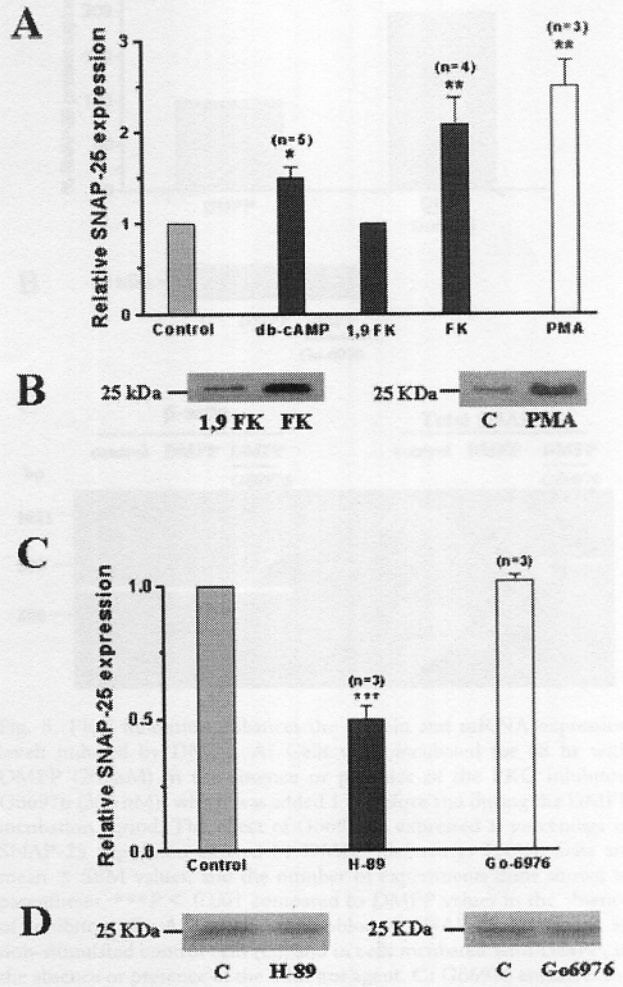

Fig. 7. PKA and PKC activators increased the basal SNAP-25 protein expression levels. **A:** Cells were incubated during 48 hr in control conditions or in the presence of PKA activators, db-cAMP (1 mM) and forskolin (10 μM), an inactive analogue of forskolin, 1,9 dideoxyforskolin (10 μM) or a PKC activator, PMA (100 ng/ml). Protein expression in the presence of PKA or PKC activators is expressed as a relative increase, compared to control (referred as 1). Data are mean ± SEM of the number of experiments shown in parentheses. $**P < 0.01$, $*P < 0.05$ compared to parallel control cells. **B:** Left panel shows a representative immunoblot of SNAP-25 expression in cells exposed to 1,9 dideoxyforskolin (1,9 FK) and forskolin (FK). Right panel shows a typical immunoblot in non-stimulated control cells (C) or in PMA-treated cells. **C:** Cells were incubated during 48 hr in control conditions or in presence of the PKA inhibitor H-89 (10 μM) or the PKC inhibitor Gö6976 (300 nM). Protein expression in the presence of the inhibitors is presented as a relative increase, compared to control (referred to as 1). Data are mean ± SEM of the number of experiments shown in parentheses. **D:** A representative immunoblot of SNAP-25 expression in control (C) and in the presence of H-89 or Gö6976.

increase in the basal SNAP-25 expression levels (1.5 ± 0.14-fold; $P < 0.05$) compared to basal values obtained in control non-incubated cells (Fig. 7A). Forskolin (FK, 10 μM), a second PKA activator, also enhanced the basal expression of SNAP-25 by 2.1 ± 0.3-fold ($n = 4$; $P < 0.01$) compared to cells treated with the inactive analogue of forskolin, 1,9 dideoxyforskolin (1,9 FK, 10 μM). Figure 7B shows a representative immunoblot of these experiments. It should be mentioned that when PKA was inhibited with H-89 (10 mM), basal expression of SNAP-25 was significantly reduced (Fig. 7C,D).

Effects of PKC Inhibition and Activation on SNAP-25 Expression

The contribution of the PKC signaling pathway in the regulation of SNAP-25 expression in chromaffin cells was evaluated using the PKC activator, PMA. As it is shown in Figure 7A, treatment of cells with PMA (100 ng/ml, 48 hr) resulted in an increase of the basal protein levels (2.5 ± 0.3-fold, $n = 3$; $P > 0.01$) compared to non-treated control cells. Figure 7B shows a representative immunoblot. Additional experiments were carried out incubating the cells with Gö6976, an inhibitor of Ca^{2+}/diacylglycerol-sensitive PKC isoforms. The incubation of the cells with Gö6976 (300 nM) for 48 hr did not modify basal expression of SNAP-25 (Fig. 7C and 7D).

A different picture was obtained when Gö6976 (300 nM) was assayed on protein expression induced by high K^+ or DMPP. In these experiments, the relative increase of SNAP-25 expression induced by K^+ or DMPP was 2.5 ± 0.3-fold ($n = 4$, $P < 0.01$) and 1.7 ± 0.1-fold ($n = 4$, $P < 0.01$), respectively, compared to parallel non-stimulated cells. Results indicate that whereas Gö6976 did not affect the increase of SNAP-25 expression induced by K^+-depolarization (data not shown), the drug enhanced the protein expression evoked by DMPP almost two-fold (Fig. 8A,B). Indeed, densitometric analysis of the PCR product corresponding to SNAP-25 mRNA revealed that DMPP treatment induced an increase of 1.92 ± 0.24 ($n = 6$; $P < 0.005$) and 2.8 ± 0.23-fold ($n = 3$; $P < 0.005$), in the absence or presence of Gö6976, respectively, compared to non-stimulated control cells (Fig. 8C).

To elucidate whether or not the last effect of Gö6976 was related to a higher influx of Ca^{2+} to the cell, we evaluated the effect of Gö6976 on the $[Ca^{2+}]_i$ response elicited by DMPP. Thus, Indo-1-loaded chromaffin cells were stimulated with successive pulses of DMPP (20 μM), in the absence or presence of Gö6976 (300 nM); the PKC inhibitor was present 30 min before and during the pulse. In these conditions, Gö6976 enhanced the $[Ca^{2+}]_i$ signal induced by DMPP by 1.65 ± 0.65-fold (Fig. 9).

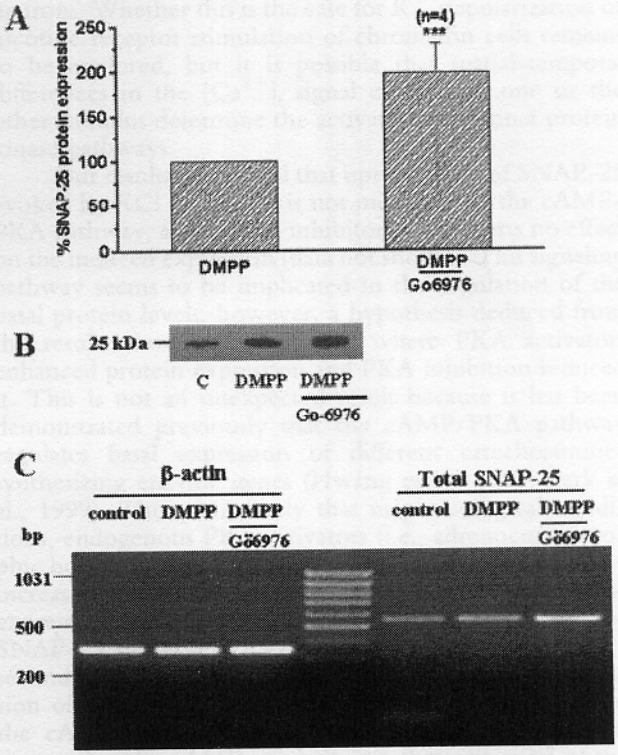

Fig. 8. PKC inhibition enhances the protein and mRNA expression levels induced by DMPP. **A:** Cells were incubated for 48 hr with DMPP (20 μM) in the absence or presence of the PKC inhibitor, Gö6976 (300 nM), which was added 1 hr before and during the DMPP incubation period. The effect of Gö6976 is expressed as percentage of SNAP-25 expression elicited by DMPP (defined as 100%). Data are mean ± SEM values, and the number of experiments done shown in parentheses. ***$P < 0.001$ compared to DMPP values in the absence of inhibitors. **B:** A typical immunoblot of SNAP-25 expression in non-stimulated control cells (C), and in cells incubated with DMPP, in the absence or presence of the inhibitor agent. **C:** Gö6976 enhances the SNAP-25 mRNA expression elicited by DMPP. Cells were incubated during 24 hr with DMPP 20μM, in the absence or presence of Gö6976; then RT-PCR of total RNA was carried out to determine, simultaneously, products corresponding to SNAP-25 and β-actin mRNAs. Aliquots (20 μl) of each PCR reaction were run on 1.5% agarose gels and stained with ethidium bromide to visualize the bands.

DISCUSSION

Previous findings from our group indicated that stimulation of chromaffin cells with high K^+ or with the nicotinic receptor agonist DMPP not only induced catecholamine secretion but also increased the expression of the protein SNAP-25 in a Ca^{2+}-dependent manner (García-Palomero et al., 2000a). Nevertheless, mechanisms governing such protein expression remain poorly known despite the essential role this protein plays in regulated exocytosis in neurons and other neuroendocrine cells. The present study was designed to give insight into the signal transduction mechanisms that regulate the expression of this protein.

By using primary cultured of bovine adrenal medullary chromaffin cells and specific inhibitors of different protein kinases, we demonstrated that CaMK is a component of high K^+ or DMPP signaling that causes upregulation of SNAP-25 expression. This conclusion was reached after observing the effect of KN-62 and KN-93 on protein and mRNA expression (Figs. 2,5). Because both CaMK inhibitors also block Ca^{2+} entry into chromaffin cells (Maurer et al., 1996; Tsutsui et al., 1996), however, their effects on SNAP-25 expression likely reflect a combined CaMK/Ca^{2+} influx inhibitory action. The last statement is supported by results shown in Figure 2 and Figure 3, where KN-93 inhibits Ca^{2+} influx as its inactive analogue KN-92, but it reduces protein expression to a value significantly higher (88% vs. 34%). At this moment, our results do not allow us to conclude which is the CaMK isoform implicated in such regulation, although one possible candidate could be the CaMK-II isoform

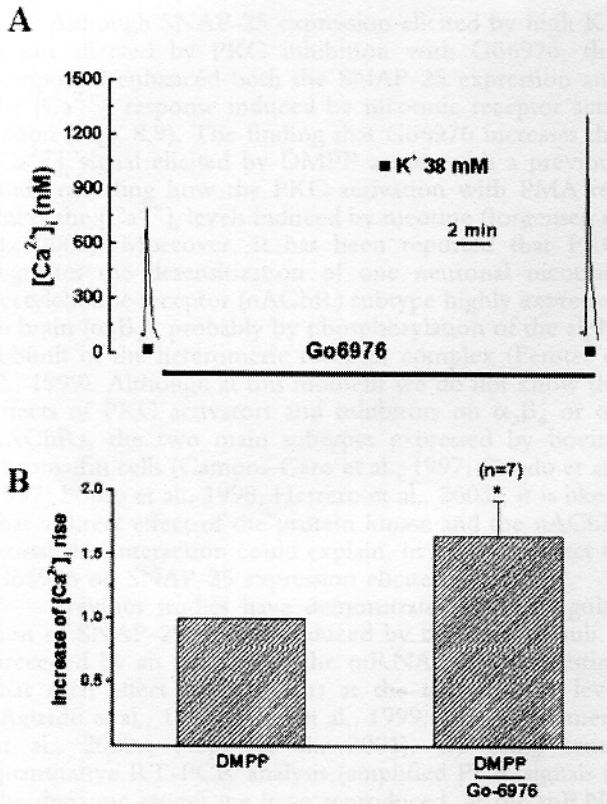

Fig. 9. The inhibitor of PKC, Gö6976, enhances the $[Ca^{2+}]_i$ signal evoked by DMPP in Indo-1-loaded single chromaffin cells. Cells were stimulated with 15-sec pulses of DMPP (20 μM), applied every 30 min. When $[Ca^{2+}]_i$ signals were reproducible, Gö6976 was added 30 min before and during the DMPP pulse. **A:** Original record of the $[Ca^{2+}]_i$ signals induced by two successive DMPP pulses (black squares at the bottom of the panel) applied in the absence or presence of Gö6976. **B:** Data, expressed as relative increase of $[Ca^{2+}]_i$ rise induced by DMPP (referred to as the unit), are mean ± SEM values obtained in the number of cells shown in parentheses.

whose expression and activation by cholinergic receptor stimulation of bovine chromaffin cells has been reported previously (Pavlovic-Surjancev et al., 1992; Tsutsui et al., 1994).

A different picture was obtained upon incubation of the cells with the MAPK inhibitors, U0126 and PD98059. We found that MAPK was involved in the upregulation of SNAP-25 expression only when cells were stimulated with high K^+ but not with DMPP. This result might be explained if different stimuli that determine increased $[Ca^{2+}]_i$ signal mediate gene expression throughout different signal transduction pathways, as it has been suggested by other authors (Bading et al., 1993; Lerea and McNamara, 1993; Brosenitsch and Katz, 2001). In fact, Bading et al. (1993) found that Ca^{2+} entry through L-type Ca^{2+} channels or *N*-Methyl-D-aspartate receptor (NMDA) recruited distinct signaling pathways that converge in the induction of the c-fos gene expression in hippocampal neurons. Whether this is the case for K^+-depolarization or nicotine receptor stimulation of chromaffin cells remains to be explored, but it is possible that spatial-temporal differences in the $[Ca^{2+}]_i$ signal elicited by one or the other stimulus determine the activation of distinct protein kinase pathways.

Our results also reveal that upregulation of SNAP-25 evoked by KCl or DMPP is not mediated by the cAMP/PKA pathway, as the PKA inhibitor H-89 exerts no effect on the induced expression (data not shown). This signaling pathway seems to be implicated in the regulation of the basal protein levels, however, a hypothesis deduced from the results shown in Figure 7, where PKA activators enhanced protein expression and PKA inhibition reduced it. This is not an unexpected result because it has been demonstrated previously that the cAMP/PKA pathway regulates basal expression of different catecholamine-synthesizing enzyme genes (Hwang et al., 1997; Park et al., 1999). Thus, it is likely that in physiological conditions, endogenous PKA activators (i.e., adrenocorticotrophic hormone, vasoactive intestinal peptide, nutrients), by increasing cAMP levels, can regulate basal SNAP-25 gene expression acting via the CRE sequence present in the SNAP-25 promoter (Ryabinin et al., 1995). Further, a second mechanism can also explain the enhanced expression of SNAP-25 in chromaffin cells upon activation of the cAMP/PKA pathway. In this manner, it has been shown that the cAMP rise increases the expression of the transcription factor Brn-3a, which in turn regulates SNAP-25 gene expression (Budhram-Mahadeo et al., 1994; Lakin et al., 1995).

The PKC is part of a multimember family of lipid-dependent, serine-threonine protein kinases, which has been implicated in the secretion of catecholamines from chromaffin cells, particularly upon nicotine receptor stimulation (Cox and Parsons, 1997). Two phorbol ester-sensitive PKC isoforms have been detected in bovine chromaffin cells (Sena et al., 1996; Yanagita et al., 2000): the PKC-α, which is activated by diacylglycerol in a Ca^{2+}-dependent manner and the PKC-ϵ, which requires diacylglycerol but not Ca^{2+} for activation. Thus, it is possible that each of these isoforms might be activated independently. This is a very interesting issue because each PKC isoform regulates voltage-sensitive Ca^{2+} and Na^+ channels in a different manner: whereas PKC-α promotes Na^+ channels internalization, PKC-ϵ decreases the half-life of the Na^+ channel α-subunit mRNA and inhibits voltage-sensitive Ca^{2+} channels (Yanagita et al., 2000, Sena et al., 2001). Our results showing that PKC activation by PMA increased basal SNAP-25 level, whereas PKC-α inhibition with Gö6976 did not (Fig. 7), suggest that in chromaffin cells the Ca^{2+}-insensitive/phorbol ester-sensitive PKC-ϵ isoform controls the basal levels of SNAP-25. This finding contrasts with previous data obtained in PC12 cells and in hippocampal explants, where PMA did not modify SNAP-25 protein expression (Sepúlveda et al., 1998). Such a discrepancy may be due to species or tissue differences in the expression profile of the Ca^{2+}-insensitive members of the PKC family.

Although SNAP-25 expression elicited by high K^+ is not affected by PKC inhibition with Gö6976, this compound enhanced both the SNAP-25 expression and the $[Ca^{2+}]_i$ response induced by nicotinic receptor activation (Figs. 8,9). The finding that Gö6976 increases the $[Ca^{2+}]_i$ signal elicited by DMPP agrees with a previous study revealing how the PKC activation with PMA reduces the $[Ca^{2+}]_i$ levels induced by nicotine (Jorgensen et al., 2000). Moreover, it has been reported that PKC regulates the desensitization of one neuronal nicotinic acetylcholine receptor (nAChR) subtype highly expressed in brain ($\alpha_4\beta_2$), probably by phosphorylation of the alpha subunit of the heteromeric receptor complex (Fenster et al., 1999). Although at this moment we do not know the effects of PKC activators and inhibitors on $\alpha_3\beta_4$ or α_7 nAChRs, the two main subtypes expressed by bovine chromaffin cells (Campos-Caro et al., 1997; Criado et al., 1997; López et al., 1998; Herrero et al., 2002), it is likely that a direct effect of the protein kinase and the nAChR exists; this interaction could explain, in part, the effect of Gö6976 on SNAP-25 expression elicited by DMPP.

Previous studies have demonstrated that upregulation of SNAP-25 protein induced by different stimuli is preceded by an increase in the mRNA level, suggesting that such effect likely occurs at the transcription level (Aguado et al., 1999; Marti et al., 1999; García-Palomero et al., 2000a; Hepp et al., 2001). By using semiquantitative RT-PCR analysis (amplified PCR signals in the dynamic range) we have reproduced, at the mRNA level, all results on protein expression obtained upon activation or inhibition of different protein kinases (Figs. 2C,5C,6C,8C).

In accordance with previous data, we find that both isoforms of SNAP-25 (a and b) are expressed constitutively in bovine chromaffin cells in culture (Fig. 1B), although the SNAP-25b is the major form expressed (Grant et al., 1999). Interestingly, this isoform has been correlated with the adrenergic phenotype, which represents around 80% of the total population of cells in cultured bovine chromaffin cells. On the other hand, we found that SNAP-25a expression is enhanced preferentially upon high K^+ or DMPP stimulation of the cells. In this regard, it has been described previously that one or the other isoform of SNAP-25 might be regulated preferentially depending on stimulus, the cell type or the species studied (Boschert et al., 1996; Roberts et al., 1998; Hepp et al., 2001). Because different authors have proposed that SNAP-25a is required for neurotransmitter release whereas SNAP-25b is involved in neurite outgrowth, it is possible that a preferential up-regulation of a particular isoform might have functional consequences. Nevertheless, more recent studies have suggested that both isoforms are implicated in the neurotransmitter secretion (Bark et al., 1995; Boschert et al., 1996, Grant et al., 1999; Puffer et al., 2001).

In conclusion, our results demonstrate that bovine chromaffin cells have significant regulatory flexibility to control the SNAP-25 expression. Such flexibility is most likely due to a set of protein kinases available to be activated selectively in particular physiological or experimental situations. Thus, depending on the isoform of protein kinase expressed by the cell, the type of stimulus used, the level or the spatial-temporal profile of the $[Ca^{2+}]_i$ signal, one or the other protein kinase might be activated preferentially. Upregulation of catecholamine biosynthetic enzyme genes by prolonged depolarization of chromaffin cells also occurs in vivo upon stressful conditions (Fluharty et al., 1983; Stachowiak et al., 1985; Richard et al., 1988; Baruchin et al., 1990). This poses the interesting question of how stressful situations influence the up-regulation of SNAP-25 in chromaffin cells and thus increase the functional efficacy of the secretory machinery.

ACKNOWLEDGMENTS

We thank Dr. P. Caviedes and Dr. A. Neely for commentaries and R. de Pascual for his invaluable help in the isolation of chromaffin cells.

REFERENCES

Aguado F, Pozas E, Blasi J. 1999. Colchicine administration in the rat central nervous system induces SNAP-25 expression. Neuroscience 93: 275–283.

Bading H, Ginty DD, Greenberg ME. 1993. Regulation of gene expression in hippocampal neurons by distinct calcium signaling pathways. Science 260:181–186.

Bark IC, Hahn KM, Ryabinin AE, Wilson MC. 1995. Differential expression of SNAP-25 protein isoforms during divergent vesicle fusion events of neural development. Proc Natl Acad Sci USA 92:1510–1514.

Baruchin A, Weisbeg EP, Mner LL, Enis D, Nisebaum LK, Naylor E, Stricker EM, Zigmond MJ, Kaplan BB. 1990. Effects of cold exposure on rat adrenal tyrosine hydroxylase: an analysis of RNA, protein, enzyme activity, and co-factor levels. J Neurochem 54:1769–1775.

Bessho Y, Nawa H, Nakanishi S. 1994. Selective up-regulation of an NMDA receptor subunit mRNA in cultured cerebellar granule cells by K^+-induced depolarization and NMDA treatment. Neuron 12:87–95.

Bito H, Deisseroth K, Tsien RW. 1996. CREB phosphorylation and dephosphorylation: a Ca^{2+}- and stimulus duration-dependent switch for hippocampal gene expression. Cell 87:1203–1214.

Boschert U, O'Shaughnessy C, Dickinson R, Tessari M, Bendotti C, Catsicas S, Pich EM. 1996. Developmental and plasticity-related differential expression of two SNAP-25 isoforms in the rat brain. J Comp Neurol 367:177–193.

Brosenitsch TA, Katz DM. 2001. Physiological patterns of electrical stimulation can induce neuronal gene expression by activating N-type calcium channels. J Neurosci 21:2571–2579.

Budhram-Mahadeo V, Theil T, Morris PJ, Lillycrop KA, Moroy T, Latchman DS. 1994. The DNA target site for the Brn-3 POU family transcription factors can confer responsiveness to cyclic AMP and removal of serum in neuronal cells. Nucleic Acids Res 22:3092–3098.

Campos-Caro A, Smillie FI, Dominguez del Toro E, Rovira JC, Vicente-Agullo F, Chapuli J, Juiz JM, Sala S, Sala F, Ballesta JJ, Criado M. 1997. Neuronal nicotinic acetylcholine receptors on bovine chromaffin cells: cloning, expression, and genomic organization of receptor subunits. J Neurochem 68:488–497.

Cárdenas AM, Allen D, Arriagada C, Olivares A, Bennett L, Caviedes R, Dagnino-Subiabre A, Mendoza IE, Segura-Aguilar J, Rapaport S, Caviedes P. 2002. Establishment and characterization of immortalized neuronal cell lines derived from the spinal cord of normal and trisomy 16 fetal mice, an animal model of Down Syndrome. J Neurosci Res 68:46–58.

Cox ME, Parsons SJ. 1997. Roles for protein kinase-C and mitogen-activated protein kinase in nicotine-induced secretion from bovine adrenal chromaffin cells. J Neurochem 69:1119–1130.

Craviso GL, Hemelt VB, Waymire JC. 1992. Nicotinic cholinergic regulation of tyrosine hydroxylase gene expression and catecholamine synthesis in isolated bovine chromaffin cells. J Neurochem 59:2285–2296.

Craviso GL, Hemelt VB, Waymire JC. 1995. The transient nicotinic stimulation of tyrosine hydroxylase gene transcription in bovine adrenal chromaffin cells is independent of c-fos gene activation. Brain Res Dev Brain Res 29:233–244.

Criado M, Dominguez del Toro E, Carrasco-Serrano C, Smillie FI, Juiz JM, Viniegra S, Ballesta JJ. 1997. Differential expression of alpha-bungarotoxin-sensitive neuronal nicotinic receptors in adrenergic chromaffin cells: a role for transcription factor Egr-1. J Neurosci 17:6554–6564.

Dass C, Mahalakshmi P. 1996. Phosphorylation of enkephalins enhances their proteolytic stability. Life Sci 58:1039–1045.

Favata MF, Horiuchi KY, Manos EJ, Daulerio AJ, Stradley DA, Feeser WS, Van Dyk DE, Pitts WJ, Earl RA, Hobbs F, Copeland RA, Magolda RL, Scherle PA, Trzaskos JM. 1998. Identification of a novel inhibitor of mitogen-activated protein kinase kinase. J Biol Chem 273:18623–18632.

Fenster CP, Beckman ML, Parker JC, Sheffield EB, Whitworth TL, Quick MW, Lester RA. 1999. Regulation of alpha4beta2 nicotinic receptor desensitization by calcium and protein kinase C. Mol Pharmacol 55:432–443.

Fluharty SJ, Snyder GL, Stricker EM, Zigmond MJ. 1983. Short- and long-term changes in adrenal tyrosine hydroxylase activity during insulin-induced hypoglycemia and cold stress. Brain Res 267:384–387.

García-Palomero E, Montiel C, Herrero CJ, García AG, Alvarez RM, Arnalich FM, Renart J, Lara H, Cárdenas AM. 2000a. Multiple calcium pathways induced the expression of SNAP-25 protein in chromaffin cells. J Neurochem 74:1049–1058.

García-Palomero E, Cuchillo-Ibañez I, García AG, Renart J, Albillos A, Montiel C. 2000b. Greater diversity than previously thought of chromaffin cell Ca^{2+} channels, derived from mRNA identification studies. FEBS Lett 481:235–239.

Grant NJ, Hepp R, Krause W, Aunis D, Oehme P, Langley K. 1999. Differential expression of SNAP-25 isoforms and SNAP-23 in the adrenal gland. J Neurochem 72:363–371.

Greber S, Lubec G, Cairns N, Fountoulakis M. 1999. Decreased levels of synaptosomal associated protein 25 in the brain of patients with Down syndrome and Alzheimer's disease. Electrophoresis 20:928–934.

Hepp R, Dupont JL, Aunis D, Langley K, Grant NJ. 2001. NGF enhances depolarization effects on SNAP-25 expression: induction of SNAP-25b isoform. Neuroreport 12:673–677.

Herrero CJ, Alés E, Pintado AJ, López AG, García-Palomero E, Mahata SK, O'Connor DT, Garcia AG, Montiel C. 2002. Modulatory mechanism of neuronal nicotinic acetylcholine receptors and exocytosis by the endogenous peptide, catestatin. J Neurosci 22:377–388.

Hiremagalur B, Nankova B, Nitahara J, Zeman R, Sabban EL. 1993. Nicotine increases expression of tyrosine hydroxylase gene. Involvement of protein kinase A-mediated pathway. J Biol Chem 268:23704–23711.

Hiremagalur B, Sabban EL. 1995. Nicotine elicits changes in expression of adrenal catecholamine biosynthetic enzymes, neuropeptide Y and immediate early genes by injection but not continuous infusion. Mol Brain Res 32:105–115.

Hwang O, Park SY, Kim KS. 1997. Protein kinase A coordinately regulates both basal expression and cyclic AMP-mediated induction of three catecholamine-synthesizing enzyme genes. J Neurochem 68:2241–2247.

Impey S, Obrietan K, Wong ST, Poser S, Yano S, Wayman G, Deloume JC, Chan G, Strom DR. 1998. Cross-talk between ERK and PKA is required for Ca^{2+} stimulation of CREB-dependent transcription and ERK nuclear translocation. Neuron 21:869–883.

Ishida N, Kitagawa M, Hatakeyama S, Nakayama K. 2000. Phosphorylation at serine 10, a major phosphorylation site of p27 (Kip1), increases its protein stability. J Biol Chem 275:25146–25154.

Jorgensen MS, Wagner PG, Arden WA, Jackson BA. 2000. Modulation of stimulus-secretion coupling in porcine adrenal chromaffin cells by receptor-mediated increases in protein kinase C activity. J Neurosci Res 59:760–766.

Kaldy P, Schmitt-Verhulst AM. 1995. Regulation of interferon-gamma mRNA in a cytolytic T cell clone: (Ca^{2+})-induced transcription followed by mRNA stabilization through activation of protein kinase C or increase in cAMP. Eur J Immunol 25:889–895.

Laemmli UK. 1970. Cleavage of structural proteins during the assembly of the head of bacteriophage T4. Nature 227:680–685.

Lakin ND, Morris PJ, Theil T, Sato TN, Moroy T, Wilson MC, Latchman DS. 1995. Regulation of neurite outgrowth and SNAP-25 gene expression by the Brn-3a transcription factor. J Biol Chem 270:15858–15863.

Lee NH, Malek RL. 1998. Nerve growth factor regulation of M4 muscarinic receptor mRNA stability but not gene transcription requires mitogen-activated protein kinase activity. J Biol Chem 273:22317–22325.

Lee MS, Zhu YL, Sun Z, Rhee H, Jeromin A, Roder J, Dannies PS. 2000. Accumulation of synaptosomal-associated protein of 25 kDa (SNAP-25) and other proteins associated with the secretory pathway in GH4C1 cells upon treatment with estradiol, insulin, and epidermal growth factor. Endocrinology 141:3485–3492.

Lerea LS, McNamara JO. 1993. Ionotropic glutamate receptor subtypes activate c-fos transcription by distinct calcium-requiring intracellular signaling pathways. Neuron 10:31–41.

Livett BG. 1984. Adrenal medullary chromaffin cells in vitro. Physiol Rev 64:1103–1161.

López MG, Montiel C, Herrero C, García-Palomero E, Mayorgas I, Hernández-Guijo JM, Villarrolla M, Gandía L, McIntosh JM, Olivera BM, García AG. 1998. Unmasking the functions of the chromaffin cell α7 nicotinic receptor by using short pulses of acetylcholine and selective blockers. Proc Natl Acad Sci USA 95:14184–14189.

Marti E, Blasi J, Gomez De Aranda I, Ribera R, Blanco R, Ferrer I. 1999. Selective early induction of synaptosomal-associated protein (molecular weight 25,000) following systemic administration of kainate at convulsant doses in the rat. Neuroscience 90:1421–1432.

Maurer JA, Wenger BW, McKay DB. 1996. Effects of protein kinase inhibitors on morphology and function of cultured bovine adrenal chromaffin cells: KN-62 inhibits secretory function by blocking stimulated Ca^{2+} entry. J Neurochem 66:105–113.

Moro MA, López MG, Gandia L, Michelena P, García AG. 1990. Separation and culture of living adrenaline- and noradrenaline-containing cells from bovine adrenal medullae. Anal Biochem 185:243–248.

Musti AM, Treier M, Bohmann D. 1997. Reduced ubiquitin-dependent degradation of c-Jun after phosphorylation by MAP kinases. Science 275:400–402.

Niki I, Okazaki K, Saitoh M, Niki A, Niki H, Tamagawa T, Iguchi A, Hidaka H. 1993. Presence and possible involvement of Ca/calmodulin-dependent protein kinases in insulin release from the rat pancreatic beta cell. Biochem Biophys Res Commun 191:255–261.

Park SY, Choi HJ, Hwang O. 1999. Regulation of basal expression of catecholamine-synthesizing enzyme genes by PACAP. Mol Cell 9:146–151.

Park JW, Jang MA, Lee YH, Passaniti A, Kwon TK. 2001. p53-independent elevation of p21 expression by PMA results from PKC-mediated mRNA stabilization. Biochem Biophys Res Commun 280: 244–248.

Pasinelli P, Ramakers GM, Urban IJ, Hens JJ, Oestreicher AB, de Graan PN, Gispen WH. 1995. Long-term potentiation and synaptic protein phosphorylation. Behav Brain Res 66:53–59.

Pavlovic-Surjancev B, Cahill AL, Perlman RL. 1992. Nicotinic agonists, phorbol esters and growth factors activate two extracellular signal-regulated kinases, ERK1 and ERK2, in bovine chromaffin cells. J Neurochem 59:2134–2140.

Puffer EB, Lomneth RB, Sarkar HK, Singh BR. 2001. Differential roles of developmentally distinct SNAP-25 isoforms in the neurotransmitter release process. Biochemistry 40:9374–9378.

Richard F, Faucon-Biguet N, Labatut R, Trollet D, Mallet J, Buda M. 1988. Modulation of tyrosine hydroxylase gene expression in rat brain and adrenals by exposure to cold. J Neurosci Res 20:32–37.

Roberts LA, Morris BJ, O'Shaughnessy CT. 1998. Involvement of two isoforms of SNAP-25 in the expression of long-term potentiation in the rat hippocampus. Neuroreport 9:33–36.

Ryabinin AE, Sato TN, Morris PJ, Latchman DS, Wilson MC. 1995. Immediate upstream promoter regions required for neurospecific expression of SNAP-25. J Mol Neurosci 6:201–210.

Sena CM, Santos RM, Boarder MR, Rosario LM. 1996. Differential regulation of histamine- and bradykinin-stimulated phospholipase C in adrenal chromaffin cells: evidence for involvement of different protein kinase C isoforms. J Neurochem 66:1086–1094.

Sena CM, Santos RM, Standen NB, Boarder MR, Rosario LM. 2001. Isoform-specific inhibition of voltage-sensitive Ca(2+) channels by protein kinase C in adrenal chromaffin cells. FEBS Lett 492:146–150.

Sepúlveda CM, Troncoso CC, Lara H, Cárdenas AM. 1998. Intracellular calcium and arachidonic acid increase SNAP-25 expression in cultured rat cerebellar explants. Neurosci Lett 252:127–130.

Stachowiak MK, Hong JS, Viveros OH. 1990. Coordinate and differential regulation of phenylethanolamine *N*-methyltransferase, tyrosine hydroxylase and proenkephalin mRNAs by neuronal and hormonal mechanism in cultured bovine adrenal medullary cells. Brain Res 510:277–288.

Stachowiak M, Sebbabe R, Stricker EM, Zigmond MJ, Kaplan BB. 1985. Effect of chronic cold exposure on tyrosine hydroxylase mRNA in rat gland. Brain Res 359:356–359.

Tang K, Wu H, Mahata SK, Mahata M, Gill BM, Parmer RJ, O'Connor DT. 1997. Stimulus coupling to transcription versus secretion in pheochromocytoma cells. Convergent and divergent signal transduction pathways and the crucial roles for route of cytosolic calcium entry and protein kinase C. J Clin Invest 100:1180–1192.

Tsutsui M, Yanagihara N, Fukunaga K, Minami K, Nakashima Y, Kuroiwa A, Miyamoto E, Izumi F. 1996. Ca^{2+}/calmodulin-dependent protein kinase II inhibitor KN-62 inhibits adrenal medullary chromaffin cell functions independent of its action on the kinase. J Neurochem 66:2517–2522.

Tsutsui M, Yanagihara N, Miyamato E, Kuroiwas A, Izumi F. 1994. Correlation of activation of Ca^{2+}/calmodulin-dependent protein kinase II with catecholamine secretion and tyrosine hydroxylase activation in cultured bovine adrenal medullary cells. Mol Pharmacol 46: 1041–1047.

Turner KM, Burgoyne RD, Morgan A. 1999. Protein phosphorylation and the regulation of synaptic membrane traffic. Trends Neurosci 22:459–464.

Yanagita T, Kobayashi H, Yamamoto R, Kataoka H, Yokoo H, Shiraishi S, Minami S, Koono M, Wada A. 2000. Protein kinase C-alpha and -epsilon down-regulate cell surface sodium channels via differential mechanisms in adrenal chromaffin cells. J Neurochem 74:1674–1684.

Young CE, Arima K, Xie J, Hu L, Beach TG, Falkai P, Honer WG. 1998. SNAP-25 deficit and hippocampal connectivity in schizophrenia. Cereb Cortex 8:261–268.

Voltammetric Behaviour of Nitrofurazone, Furazolidone and Other Nitro Derivatives of Biological Importance

Alfonso Morales, Pablo Richter and M. Inés Toral
Department of Chemistry, Faculty of Sciences, University of Chile, Las Palmeras 3425, P.O. Box 653, Santiago, Chile

In pyridine - formic acid buffer and tetramethylammonium chloride solution of pH 4.5 at a dropping mercury or a glassy carbon electrode, nitrofurazone, furazolidone and nitrofurantoin are reduced in a single six-electron wave, while chloramphenicol and other structurally related nitro derivatives are reduced in only one four-electron wave, the nitro group being reduced to the amine or to the hydroxylamine, respectively. The electrochemical behaviour of these compounds depends mainly on the nature and position of the substituents. Reduction to the primary amine occurs when the substituents possess available π electrons to conjugate with the nitro group of the aromatic ring, which determines the transformation of the hydroxylamine into the amine via formation of a highly reducible intermediate imine or a quinonoid structure. In contrast, if the formation of the intermediate imine is made impossible by an adverse effect of the substituent, the hydroxylamine does not undergo further reduction.

Cyclic voltammograms were recorded at different pH values and at different scan rates in order to identify certain relatively unstable species. The effect of pH on the diffusion-limited current and on the $E_{\frac{1}{2}}$ values of the polarographic waves was also studied and the results obtained were compared with those obtained by cyclic voltammetry.

On this basis, and according to the polarographic and cyclic voltammetric data, a reduction mechanism for the nitrofuran derivatives is suggested, in which the importance of the homogeneous chemical reactions associated with the electron-transfer steps is examined.

Keywords: *Nitrofurazone, furazolidone and chloramphenicol; nitro derivatives of 1,4-benzodiazepines; polarography; cyclic voltammetry*

Nitrofurazone (**I**), furazolidone (**II**) and nitrofurantoin (**III**) are structurally related, with a nitro group at the 5-position on the furan ring. The electrochemical behaviour of these nitrofurans and other aromatic nitro derivatives such as chloramphenicol, clonazepam, nitrazepam, flunitrazepam and parathion is based on the ease of reduction of the nitro group at a dropping mercury or solid electrode.

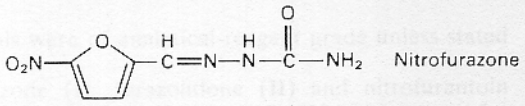

Nitrofurazone

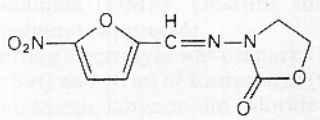

Furazolidone

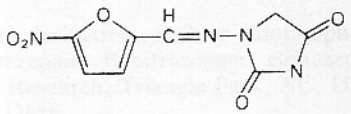

Nitrofurantoin

Polarography has been widely used in order to elucidate the reduction mechanism at a dropping mercury electrode and to investigate the resemblance with the metabolic pathway for the biological degradation of these nitro derivatives. These compounds are generally metabolised *in vivo* to the corresponding amines via nitroso and hydroxylamine intermediates. However, the polarographic techniques cannot determine these metabolites owing to the ill-defined reduction wave of the hydroxylamine, the inability of the amine group to react at the dropping mercury electrode and because the reduction of the nitroso group to hydroxylamine occurs at a more positive potential than the reduction potential of the nitro group to hydroxylamine, and consequently that reduction wave is not detected. Further, the variable number of reduction waves for each compound, depending on the supporting electrolyte, pH and maximum supressors employed, illustrates the complexity of the electrode processes involved. In Britton - Robinson buffer at pH values below 5, the nitro group of the nitrofurantoin is reduced to hydroxylamine in a four-electron process and subsequently to the amine in a two-electron process.[1] Similarly, nitrofurazone shows a two-step reduction wave in different supporting electrolytes, the second wave being attributed to a simultaneous reduction of the hydroxylamine and the azomethine group.[2]

The determination of some nitrated neterocyclic compounds containing similar types of reduction sites to that of nitrofurazone was studied earlier by Vignoli *et al.*,[3] using a Britton - Robinson buffer of pH between 1.81 and 11.98. They observed two waves for the reduction of the nitro group and three waves at lower pH values when the compounds had a substituted imino group.

A polarographic method has been used to determine furazolidone in feed pre-mixes,[4] but little attention has been paid to the electrochemical behaviour of this compound.

In previous polarographic work[5] in which a solvent - buffer system containing pyridine and formic acid in conjunction with tetramethylammonium chloride solution was used as the supporting electrolyte, it was found that the nitro group of the nitrofurantoin shows only one reduction wave corresponding to a six-electron process, and that chloramphenicol and other structurally related compounds are reduced in a single four-electron wave.

The aim of this work was to study the electrochemical behaviour of molecules having the same electroactive group in order to elucidate the effects of the nature and position of the substituents on the reduction. Significant aspects involved in

Table 1. Voltammetric data for reduction of **I** and **II** in pyridine - formic acid with TMAC as supporting electrolyte

Compound	Scan rate/ V s^{-1}	i_p/μA	$i_p/Cv^{\frac{1}{2}}$
0.196 mM **I**	0.020	5.60	202
	0.050	9.20	210
	0.100	13.20	213
	0.200	17.60	201
	0.300	20.80	194
	0.400	23.60	191
0.476 mM **I**	0.020	14.4	214
	0.050	22.4	211
	0.100	33.2	220
	0.200	43.2	203
	0.300	51.6	198
	0.400	59.2	197
0.196 mM **II**	0.120	5.8	209
	0.050	9.2	210
	0.100	12.8	207
	0.200	18.0	205
	0.300	21.6	201
	0.400	24.2	195
0.476 mM **II**	0.020	14.4	214
	0.050	22.4	211
	0.100	32.0	213
	0.200	44.2	212
	0.300	55.2	212
	0.400	60.4	201

Table 2. Polarographic data for the reduction of nine nitro compounds (0.124 mM) in pyridine - formic acid with TMAC as supporting electrolyte

Compound	No. of runs	$E_{\frac{1}{2}}$/V	i_d/μA
p-Nitrophenol	7	−0.50	2.38
Nitrofurantoin	8	−0.16	2.27
Nitrofurazone	7	−0.18	2.30
Furazolidone	7	−0.17	2.29
Chloramphenicol	9	−0.41	1.62
Nitrazepam	5	−0.34	1.62
Flunitrazepam	6	−0.28	1.55
Clonazepam	7	−0.28	1.58
Parathion	8	−0.32	1.64

the reduction were examined, together with the homogeneous chemical reactions accompanying the electrode process.

Experimental

Reagents

All chemicals were of analytical-reagent grade unless stated otherwise.

Nitrofurazone (**I**), furazolidone (**II**) and nitrofurantoin (**III**) (Sigma Chemical, St. Louis, MO, USA) were used for the basic studies. Standard solutions (1.0×10^{-2} M) were prepared by dissolving the appropriate amount of each drug in dimethylformamide (DMF). Gelatine solution (0.5%) was used as a maximum suppressor.

The supporting electrolyte was prepared by diluting 20 ml of pyridine (12.3 M) and 10 ml of formic acid (98–100%) with 120 ml of 0.1 M tetramethylammonium chloride (TMAC) solution. The resulting solution had a pH of 4.5. On varying the ratio of formic acid to pyridine the pH could be varied over the range 2.6–5.1.[5]

Other nitro derivatives, such as chloramphenicol, *p*-nitrophenol, nitrazepam, flunitrazepam, clonazepam and parathion (EPA Research, Triangle Park, NC, USA), were also dissolved in DMF.

Apparatus

Polarographic assays were performed using a Polariter PO4 instrument (Radiometer, Copenhagen, Denmark). A dropping mercury electrode was used as the working electrode and a saturated calomel electrode (SCE) as the reference electrode.

Cyclic voltammetric experiments were performed using a CV-27 voltammograph (Bioanalytical Systems, Lafayette, IN, USA). A three-electrode assembly was used for all measurements. Glassy carbon was employed as working electrode, an SCE as the reference electrode and a platinum coil as the counter electrode.

An Orion Research Digital Ion-Analyzer 701 with glass and SCE electrodes was used for pH determinations.

Techniques

Aliquots of the standard solutions were diluted with the supporting electrolyte, de-oxygenated with oxygen-free nitrogen and analysed using the d.c. polarographic mode. The mercury flow-rate, m, and the drop time, t, were determined at various heights of the mercury column, h. The diffusion-controlled character of the current and the dependence of the diffusion-limited current on the depolariser concentration were established.

Cyclic voltammetric experiments were carried out under identical experimental conditions. All measurements were performed at 25 ± 1 °C. Dissolved air was removed from the solutions by bubbling oxygen-free nitrogen through the cell for 10 min, then passing it over the solution during the electrolysis. Voltammograms were recorded at scan rates between 0.02 and 0.4 V s^{-1}. The current function $i_p/Cv^{\frac{1}{2}}$ was found to be fairly constant for **I** and **II** (Table 1).

pH Studies

The effects of pH on the half-wave potentials and diffusion-limited current for **I** and **II** at a concentration 0.124 mM were studied over the pH range 1–14. The corresponding voltammograms were recorded under identical conditions.

Results and Discussion

Under the experimental conditions described above, the polarographic reduction of some aromatic nitro compounds of biological importance was found to give rise either to a single well defined wave corresponding to a six-electron process or to a single wave corresponding to a four-electron process. The electrochemical behaviour depends on the nature of the aromatic ring and on the nature and position of the substituents. When a solvent - buffer system (pH 4.5) containing pyridine and formic acid in conjunction with tetramethylammonium chloride solution was used as the supporting electrolyte, compounds containing a nitro-substituted furan ring behave as *p*-nitrophenol and are reduced to the corresponding amine in a six-electron reaction in a single step. Reduction of such compounds, except *p*-nitrophenol, occurs at relatively lower negative potentials than that of other nitro compounds, which indicates some nitroso character (Table 2). When equimolar solutions of **I**–**III** were polarographed using the supporting electrolyte mentioned above, the ratio of wave heights was approximately 1.00 ± 0.04, indicating a reduction process similar to that for the corresponding primary amine (Fig. 1). Using controlled potential electrolysis, Mishra and Gode[2] recently demonstrated that the ultimate reduced product of nitrofurazone is the primary amine.

Reduction by six electrons in a single step occurs only if the substituents possess available π electrons to conjugate with

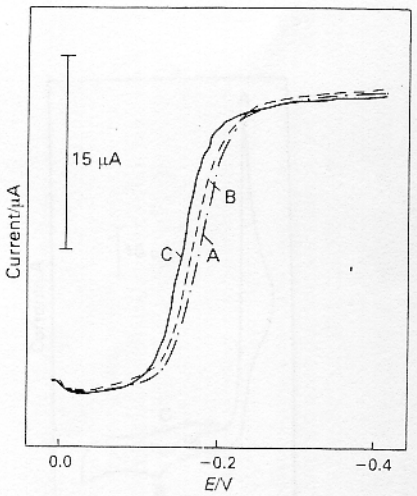

Fig. 1. Polarographic reduction waves of nitrofurazone, furazolidone and nitrofurantoin, each at 0.124 mM. (A) Nitrofurazone: $E_{\frac{1}{2}}$ −0.18 V and i_d 2.3 μA. (B) furazolidone: $E_{\frac{1}{2}}$ −0.17 V, i_d 2.29 μA. (C) Nitrofurantoin: $E_{\frac{1}{2}}$ −0.16 V, i_d 2.27 μA. V_i = 0.00 V

the nitro group of the aromatic ring, which makes the transformation of the hydroxylamine into the imine or a quinonoid structure possible. This substituted donor group must be located at the 2-position on the furan ring or in a *para* or *ortho* position on the benzene ring in order to achieve the interaction of the π systems of the aromatic ring and of the substituents with the intermediate hydroxylamine to give the corresponding imine, which is then reduced to the primary amine.

Electrochemical reduction of **I–III** in a single wave can be explained regardless of the electron transfer process by the extremely fast chemical reactions occurring, owing to the presence of the moiety >C=N–N<. The following scheme represents the mechanism of formation of the corresponding imine from the intermediate hydroxylamine.

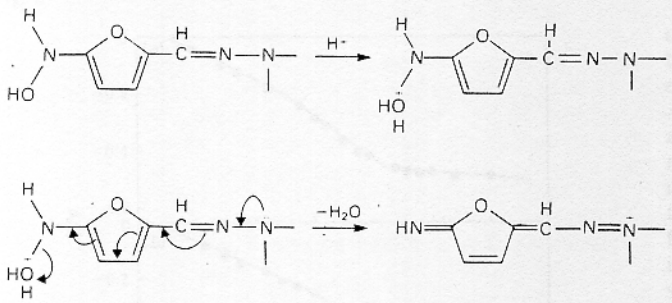

p-Nitrophenol, *p*-nitroaniline, nitrosophenols and other aromatic nitro compounds containing similar types of reduction sites and a donor group substituent show analogous polarographic behaviour.[5–9]

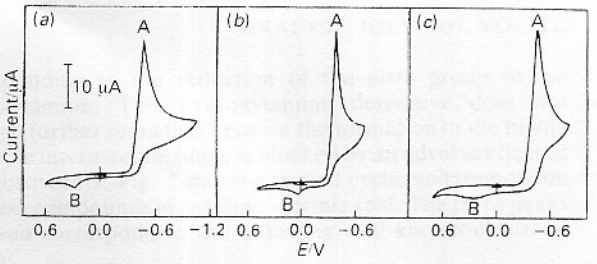

Fig. 2. Cyclic voltammograms of (*a*) nitrofurazone; (*b*) furazolidone; and (*c*) nitrofurantoin, each at 0.476 mM. pH, 4.5. Glassy carbon electrode. Scan rate. 0.1 V s^{-1}

Cyclic voltammograms of the nitrofuran derivatives (Fig. 2) were recorded under identical conditions, in order to identify intermediate species. In all instances the scan is initiated in a negative direction from 0.0 V. The initial reduction peak A corresponds to a six-electron reduction of the nitro group to the amine derivative, as shown below.

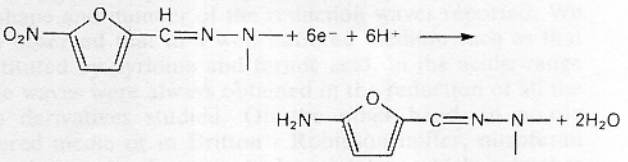

The amine thus produced is subsequently oxidised in the reverse scan at peak B to the imine or quinonoid structure intermediate. This imine is hydrolysed to a quinone derivative, which is neither oxidised nor reduced at these potentials, as shown in Scheme 1.

It can be observed that the electron transfer precedes the chemical reaction (EC reaction). Similar behaviour has been shown to occur in the oxidation of *p*-aminophenol at a platinum electrode in aqueous solutions.[10,11] Wave clipping, that is, reversal of the scan direction before peak A, causes peak B to disappear, indicating that peak B is the oxidation product of the primary amine previously formed in A.

At scan rates higher than 0.3 V s^{-1} a second cathodic peak C appears (Fig. 3), indicating that a reversible reduction of the imine derivative occurs, and that the hydrolysis of this imine is too slow to affect the reduction process. In other words, if the scan rate is very high relative to k, very little imine will be lost to the succeeding hydrolysis reaction and the electrochemical process will be reversible (see Fig. 3). Conversely, if the scan rate is low relative to k, the chemical reaction will be essentially over before the voltage scan is reversed, and the electrode process will appear totally irreversible.

The reduction potential of the highly reducible intermediate imine is more positive than the reduction potential of the nitro group to amine (peak A) and consequently this wave is not observed in normal d.c. polarography.

On the other hand, it was observed that chloramphenicol,[5,12–14] nitrazepam,[15] flunitrazepam and parathion show a different voltammetric behaviour to the nitrofuran derivatives. The former are reduced in a single four-electron wave

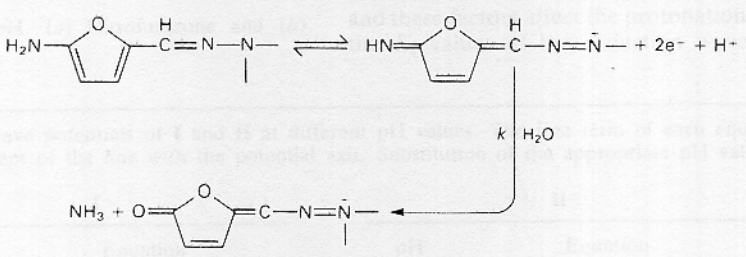

Scheme 1

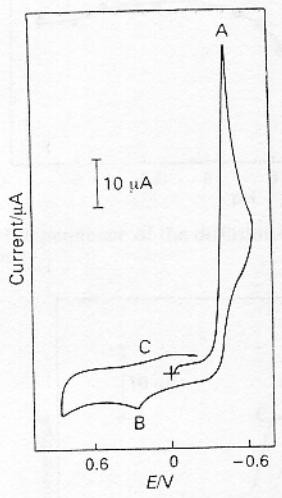

Fig. 3. Cyclic voltammogram of nitrofurazone. Scan rate, 0.3 V s^{-1}; other conditions as in Fig. 2

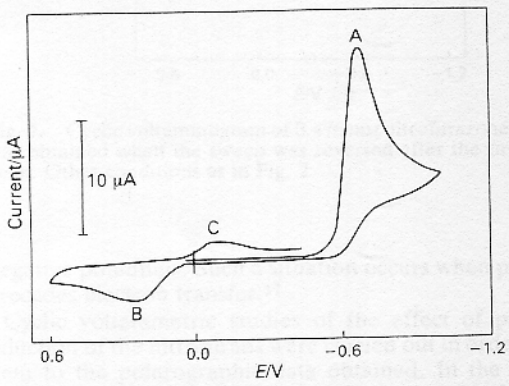

Fig. 4. Cyclic voltammogram of chloramphenicol. Conditions as in Fig. 2

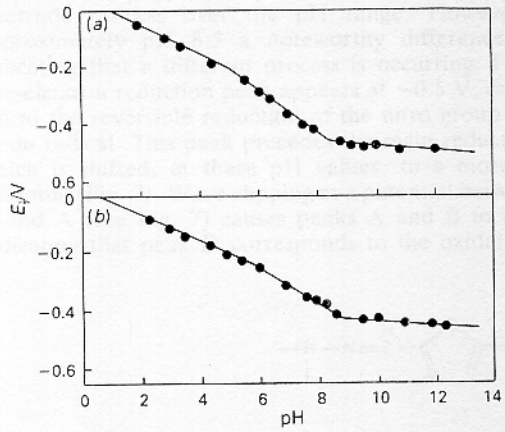

Fig. 5. Variation of $E_{\frac{1}{2}}$ with pH. (*a*) Nitrofurazone and (*b*) furazolidone, each at 0.124 mM

corresponding to the reduction of the nitro group to the hydroxylamine. This hydroxylamine derivative does not undergo further reduction because the formation of the highly reducible intermediate imine is blocked by an adverse effect of the substituents. Fig. 4 shows a typical cyclic voltammogram for these compounds in pyridine - formic acid. The three peaks observed correspond to the following well known electrode process:

Peak A: $ArNO_2 + 4e + 4H^+ \rightarrow ArNHOH + H_2O$
Peak B: $ArNHOH \rightarrow ArNO + 2e + 2H^+$
Peak C: $ArNO + 2e + 2H^+ \rightarrow ArNHOH$

Kissinger and Heineman[16] showed that the three peaks observed in the voltammogram of chloramphenicol in an acetate buffer system and using a carbon paste electrode involve more than a simple electron transfer. The irreversibility of peak A is due to the slow electron transfer occurring in the step nitro → nitroso derivative.[12–15]

In addition to these aspects, the buffer constituents of the supporting electrolyte also seem to have a significant effect on the shape and number of the reduction waves reported. We have observed that in a well buffered medium such as that constituted by pyridine and formic acid, in the acidic range single waves were always obtained in the reduction of all the nitro derivatives studied. On the other hand, in poorly buffered media or in Britton - Robinson buffer, nitrofuran derivatives are reduced to hydroxylamine, which is further reduced to the amine in a second separate wave.[1–3] According to Hess,[12] chloramphenicol is reduced in two steps in phthalate buffer of pH 4 and a similar reduction in two separate waves in acetate media has been reported.[13]

pH Studies

In d.c. polarography, the half-wave potentials for **I** and **II** are pH dependent and are shifted cathodically with increasing pH. The $E_{\frac{1}{2}}$ *versus* pH graph (Fig. 5) shows three linear portions. The equations that describe the variations of $E_{\frac{1}{2}}$ with pH were deduced from the graph and are given in Table 3.

The diffusion-limited current for both compounds is also pH dependent (Fig. 6). The slight decrease in the wave height below pH 3 is probably associated with an acid - base equilibrium as previously reported for nitrofurantoín.[1,5] Above pH 5.0 the wave slowly begins to decay for **I** and **II**, and at this pH the first break on the $E_{\frac{1}{2}}$ *versus* pH graph occurs, representing the pH at which the hydroxylamine intermediate in the reduction of the nitro group is no longer protonated and therefore cannot be easily reduced. At approximately pH 8.5 for **I** and at pH 8.8 for **II**, each wave falls sharply and breaks up into two waves. This fall is accompanied by a change in the slope of the $E_{\frac{1}{2}}$ *versus* pH graph, indicating that a different electrode process occurs. Therefore, for all these compounds the best defined and differentiated waves for analytical purposes were obtained at $3 < pH < 5$. The scission of the polarographic wave and the change in the slope of the $E_{\frac{1}{2}}$ *versus* pH graph observed at pH 8–9 can be related to the cyclic voltammetric behaviour. Possibly an increase in pH increases the dissociation constant of the protonated species and these factors affect the protonation rate and consequently the $E_{\frac{1}{2}}$ values of the reduction wave are shifted to more

Table 3. Equations of the half-wave potentials of **I** and **II** at different pH values. The first term of each equation is the slope of the line and the second is the intercept of the line with the potential axis. Substitution of the appropriate pH value will give the $E_{\frac{1}{2}}$ value at that pH

I		**II**	
pH	Equation	pH	Equation
0.0–5.12	$E_{\frac{1}{2}} = -0.051pH + 0.050V$	0.0–5.5	$E_{\frac{1}{2}} = -0.045pH + 0.024V$
5.12–8.43	$E_{\frac{1}{2}} = -0.075pH + 0.173V$	5.5–8.79	$E_{\frac{1}{2}} = -0.061pH + 0.112V$
8.43–14	$E_{\frac{1}{2}} = -0.0089pH - 0.384V$	8.79–14	$E_{\frac{1}{2}} = -0.0080pH - 0.354V$

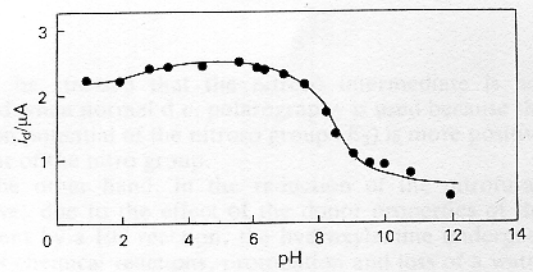

Fig. 6. pH dependence of the diffusion-limited current of 0.124 mM nitrofurazone

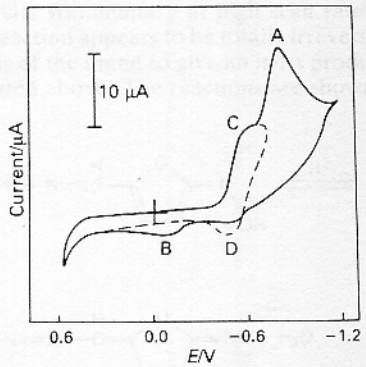

Fig. 7. Cyclic voltammogram of 0.476 mM nitrofurazone at pH 10. D was obtained when the sweep was reversed after the first reduction peak. Other conditions as in Fig. 2

negative potentials. Such a situation occurs when protonation precedes electron transfer.[17]

Cyclic voltammetric studies of the effect of pH on the reduction of the nitrofurans were carried out in order to relate them to the polarographic data obtained. In the pH range 1–8.5 no difference was observed in the shape of the cyclic voltammetric waves (Fig. 2), except that the potentials were shifted cathodically as the pH increased, indicating a similar electrode process over the pH range. However, above approximately pH 8.5 a noteworthy difference appears, indicating that a different process is occurring. For **I–III** a one-electron reduction peak appears at −0.5 V, corresponding to the reversible reduction of the nitro group to a nitro anion radical. This peak precedes the main reduction wave, which is shifted, at these pH values, to a more negative potential (Fig. 7). Wave clipping at a potential between peaks C and A (see Fig. 7) causes peaks A and B to disappear, indicating that peak D corresponds to the oxidation of the anion radical formed in C. The existence of this relatively stable anion radical in alkaline media has been recently reported in the reduction of nitrobenzene when platinum, gold and glassy carbon electrodes were used.[18] The formation of the nitro anion radical can be explained by delocalisation of the electrons in the aromatic ring due to the low proton activity in the bulk of the solution. Detection of the nitro anion radical is possible only through cyclic voltammetry.

Mechanism of the Electrode Process

Based on the polarographic and cyclic voltammetric studies, a reduction mechanism for **I–III** can be proposed. The nature of the waves and peaks was found to be diffusion controlled in the supporting electrolyte used, as shown by the $i_{lim}h^{-\frac{1}{2}}$ and $i_p/Cv^{\frac{1}{2}}$ relationships.

The irreversibility of the electrode process was verified by logarithmic analysis of the wave. The slope of the *E versus* log $(i/i_d - i)$ graph exceeds appreciably $59/n$ mV and the numerical value of $E_{\frac{1}{4}} - E_{\frac{3}{4}}$ exceeds $54.6/n$ mV.[19]

The αn_a values (where α is the transfer coefficient) and the number of protons (p values) corresponding to the rate-determining step were calculated for **I** and **II** at selected pH values. At pH 4.5 the αn_a values for **I** and **II** were found to be 1.23 and 1.15, respectively, indicating that two electrons take part in the rate-determining step of the reaction.

From the equation:

$$\frac{dE_{\frac{1}{4}}}{dpH} = \frac{-0.059}{\alpha n_a} \cdot p$$

p was found to be 0.93 and 0.88 for **I** and **II**, respectively, showing that one proton is involved in the rate-determining step of the reaction over the pH range 1–8. The participation of the hydrogen ion in the rate-determining step is due to protonation of the nitro group to form a more readily reducible species, which is reduced to the nitroso intermediate (CE reaction). A similar stoicheiometry of the rate-determining step for the reduction of nitroxazepine hydrochloride has been reported recently (Scheme 2).[20]

The nitroso intermediate group is rapidly reduced to the hydroxylamine, which is stabilised at this stage whenever the fast chemical reactions that would allow the transformation of this hydroxylamine into the highly reducible intermediate imine are inhibited. This inhibition takes place when the substituent does not have donor properties, in which event a four-electron reduction occurs. This was observed in compounds such as chloramphenicol, parathion, nitro derivatives of 1,4-benzodiazepines and other structurally related substances (CEE reaction). The nitroso - hydroxylamine reversible couple can be detected by cyclic voltammetry only when the hydroxylamine is the ultimate reduction product (Fig. 4).

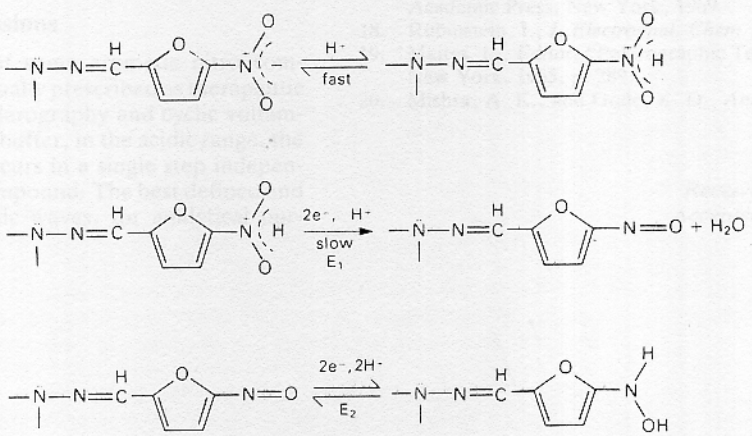

Scheme 2

It must be stressed that the nitroso intermediate is not observed when normal d.c. polarography is used because the reduction potential of the nitroso group (E_2) is more positive than that of the nitro group.

On the other hand, in the reduction of the nitrofuran derivatives due to the effect of the donor properties of the substituent by a EC reaction, the hydroxylamine undergoes very fast chemical reactions, protonation and loss of a water molecule, giving rise to the highly reducible intermediate imine, which is then reduced to the primary amine in a reversible process (Fig. 3). This reversible couple was observed by cyclic voltammetry at high scan rates. At slow scan rates this reaction appears to be totally irreversible owing to the hydrolysis of the imine to give an inert product (Figs. 2 and 3) as indicated above. The reactions are shown below.

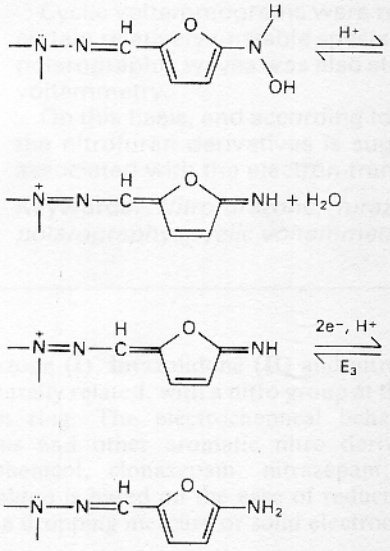

It must be noted that the potential E_3 is more positive than E_1 and therefore only one wave is observed. It may be concluded that the hydrolysis of the imine derivative is too slow to affect the polarographic wave. The above-mentioned processes, as already stated, take place in a well buffered medium of pH 4.5. In the pH range 9–14 the potentials of **I** and **II** are shifted cathodically and one reversible couple appears, at more positive potentials, corresponding to the reversible reduction of the nitro group to a nitro anion radical derivative (Fig. 7).

Conclusions

The voltammetric behaviour of some aromatic nitro compounds of biological interest, usually prescribed as therapeutic agents, has been studied by polarography and cyclic voltammetry. In pyridine - formic acid buffer, in the acidic range, the reduction of the nitro group occurs in a single step independently of the structure of the compound. The best defined and differentiated d.c. polarographic waves, for analytical purposes, were obtained at $3 < pH < 5$. As is apparent from Table 2, the difference in the half-wave potentials makes the simultaneous determination of different nitro derivatives possible.

Cyclic voltammetry was used to identify certain intermediates, metabolites and final products when reducing, under similar conditions, nitro derivatives having different substituents. Hence the formation of the intermediate nitroso group in the reduction of the nitro compounds, which are reduced to hydroxylamine, has been clearly demonstrated, together with the formation of the intermediate imine when the nitro compounds are reduced to amines. The donor properties of the substituent drive the reduction completely to the primary amine, whereas a substituent that is not a donor promotes reduction to hydroxylamine.

Cyclic voltammetry also proved to be useful for the diagnosis of the electrode reactions that are coupled with homogeneous chemical reactions.

Support from the Department of Investigation (DIB) of the University of Chile is gratefully acknowledged.

References

1. Burmicz, J. S., Smyth, W. F., and Palmer, R. F., *Analyst*, 1976, **101**, 986.
2. Mishra, A. K., and Gode, K. D., *Analyst*, 1985, **110**, 1373.
3. Vignoli, L., Cristau, B., Gouezo, F., and Fabre, C., *Chim. Anal. (Paris)*, 1963, **45**, 439.
4. Slamnik, M., *Talanta*, 1974, **21**, 960.
5. Morales, A., Toral, M. I., and Richter, P., *Analyst*, 1984, **109**, 633.
6. Chodkowski, J., and Gralewska-Ludwicka, D., *Pol. J. Chem.*, 1980, **54**, 567.
7. Stočesová, D., *Collect. Czech. Chem. Commun.*, 1949, **14**, 615.
8. Testa, A. C., and Reinmuth, W. H., *J. Am. Chem. Soc.*, 1960, **83**, 784.
9. Nicholson, R. S., and Shain, I., *Anal. Chem.*, 1965, **35**, 190.
10. Shearer, C. M., Christenson, K., Mukherji, A., and Papariello, G. J., *J. Pharm. Sci.*, 1972, **61**, 1627.
11. Bard, A. J., and Faulkner, L. R. "Electrochemical Methods. Fundamentals and Applications," Wiley, New York, 1980.
12. Hess, G. B., *Anal. Chem.*, 1950, **22**, 649.
13. Fossdal, K., and Jacobson, E., *Anal. Chim. Acta*, 1971, **56**, 105.
14. Van Der Lee, J. J., Van Bennekom, W. P., and De Jong, H. J., *Anal. Chim. Acta*, 1980, **117**, 171.
15. Halvorsen, S., and Jacobsen, E., *Anal. Chim. Acta*, 1972, **59**, 27.
16. Kissinger, P. T., and Heineman, W. R., *J. Chem. Educ.*, 1983, **60**, 702.
17. Zuman, P., "The Elucidation of Organic Electrode Processes," Academic Press, New York, 1969.
18. Rubinstein, I., *J. Electroanal. Chem.*, 1985, **183**, 379.
19. Meites, L., *Editor*, "Polarographic Techniques," Interscience, New York, 1965, p. 289.
20. Mishra, A. K., and Gode, K. D., *Analyst*, 1985, **110**, 31.

Paper A6/415
Received October 30th, 1986
Accepted February 12th, 1987